



저작자표시-비영리-동일조건변경허락 2.0 대한민국

이용자는 아래의 조건을 따르는 경우에 한하여 자유롭게

- 이 저작물을 복제, 배포, 전송, 전시, 공연 및 방송할 수 있습니다.
- 이차적 저작물을 작성할 수 있습니다.

다음과 같은 조건을 따라야 합니다:



저작자표시. 귀하는 원저작자를 표시하여야 합니다.



비영리. 귀하는 이 저작물을 영리 목적으로 이용할 수 없습니다.



동일조건변경허락. 귀하가 이 저작물을 개작, 변형 또는 가공했을 경우에는, 이 저작물과 동일한 이용허락조건하에서만 배포할 수 있습니다.

- 귀하는, 이 저작물의 재이용이나 배포의 경우, 이 저작물에 적용된 이용허락조건을 명확하게 나타내어야 합니다.
- 저작권자로부터 별도의 허가를 받으면 이러한 조건들은 적용되지 않습니다.

저작권법에 따른 이용자의 권리는 위의 내용에 의하여 영향을 받지 않습니다.

이것은 [이용허락규약\(Legal Code\)](#)을 이해하기 쉽게 요약한 것입니다.

[Disclaimer](#)

Thesis for the Degree of Master of Engineering

**Controller System Design of Two Wheeled
Mobile Inverted Pendulum**



**By
Chetanraj D. Patil**

**Department of Interdisciplinary Program of
Mechatronics Engineering, The Graduate School,
Pukyong National University**

February 2013

Controller System Design of Two Wheeled Mobile Inverted Pendulum

이륜 이동도립진자의 제어기 시스템 설계

By

Chetanraj D. Patil

Advisor: Professor Sang Bong Kim

**A thesis Submitted in Partial Fulfillment of the
Requirements for the Degree of**

Master of Engineering

**To the Department of Interdisciplinary Program of
Mechatronics Engineering, The Graduate School,
Pukyong National University**

February 2013

Controller System Design of Two Wheeled Mobile Inverted Pendulum

A thesis

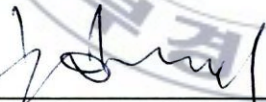
By

Chetanraj D. Patil

Approved as to styles and contents by:



Prof. Young Seok Jung
Chairman



Prof. Soon Jae Kwon
Member

Prof. Sang Bong Kim
Member



February 2013

Acknowledgements

First and foremost, I would like to express my deepest appreciation to my thesis adviser, professor, Dr. Sang Bong Kim, whose inspiration, support and perseverance made this dissertation become possible. For the last two years, Prof. Kim has been the adviser, financial supporter, mentor and guardian to me. His insight suggestions and instructions helped me to establish the direction of my research, and finish this thesis. I will always cherish these years in CIMEC Lab with his leading.

I would like to thank the members of my thesis committee: Prof. Young Seok Jung and Prof. Soon Jae Kwon for their considerable helpful comments and suggestions.

I am very much grateful to Prof. Hak Kyeong Kim for his guidance, enlightening discussions and tremendous encouragement towards me during working time in Korea. I could not finish my thesis soon without his great help during a long time working together.

I would like to acknowledge all members of CIMEC laboratory: Mr. Giang Hoang, Mr. Phuc Thinh Doan, Mr. Bui Thanh Luan, Mr. Dinh Viet Tuan from Vietnam, Mr. Seo Kwang Kim, Mr. Woo Young Jeong, Mr. Jeong Geun Kim, Miss Yu Mi Park, Miss Bae Min Ji from South Korea, Mr. Pandu Sandi Pratama from Indonesia, Mr. Waleed M.A. Elhalwagy from Egypt and all undergraduate students for all scientific discussions and helps. I also wish to express my thanks to all Indian students in Pukyong National University.

Special thank to Gitanjali Patil for being constant source of moral support and encouragement, and for always becoming my shoulder whenever I needed. Without you, my dream of completing my dissertation would have not come true.

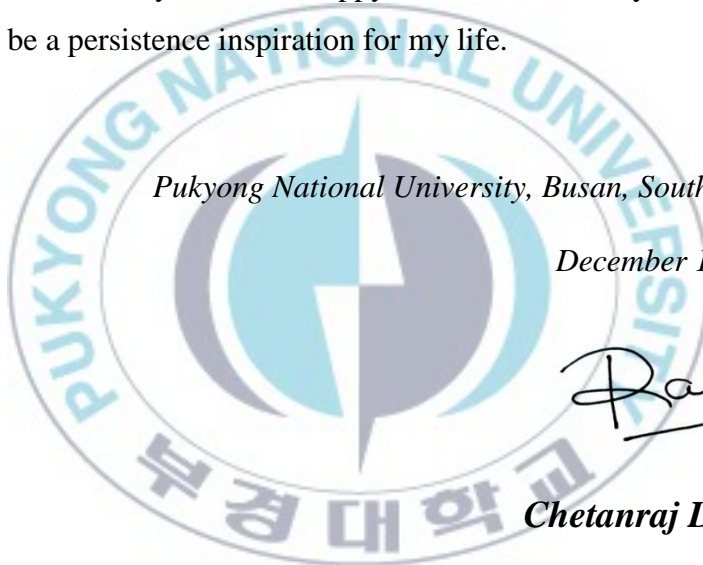
Finally, I would like to thank my parents, Rekha D. Patil and D. R. Patil, my younger brother Kashyap Patil, my best friend Satish Patil and his wife Harsha S. Patil and my entire close relative for their invaluable love and support not only in the dissertation time but also in the whole of my life. The happy memories with my family will always be a persistence inspiration for my life.

Pukyong National University, Busan, South Korea.

December 11, 2012



Chetanraj D. Patil



Contents

Acknowledgements

Abstract..... iii

List of Figures..... v

List of Tables v

Chapter 1: Introduction 1

1.1 Motivation and Background 1

1.2 Literature Review..... 3

1.3 Objective and Researching Method 7

1.4 Outline of thesis and summary of contributions 8

Chapter 2: System Description and System Modeling..... 10

2.1 System Description 10

2.2 System Modeling 19

2.2.1 Characterization of Wheels 22

2.2.2 Body Dynamics 25

Chapter 3: Controller System Design 30

3.1 Backstepping Controller Design 30

3.1.1 Balance Controller Design 31

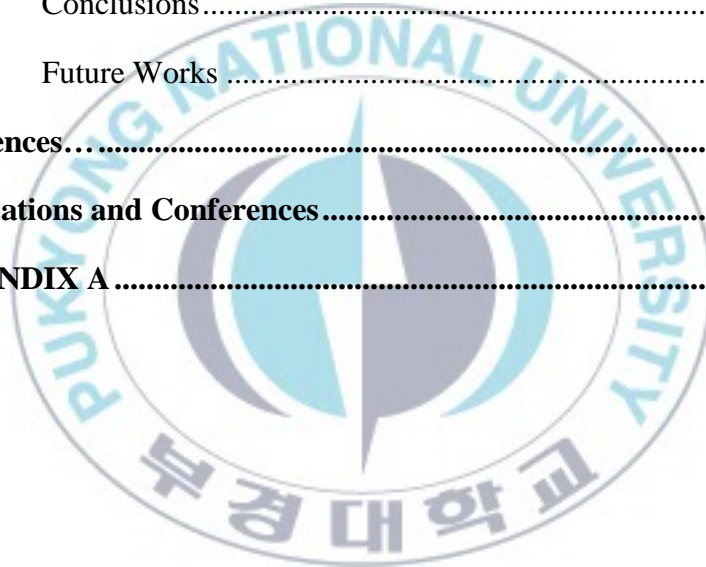
3.1.2 Rotation Controller Design 33

3.2 PD Controller Design..... 34

3.2.1 Position Controller Design 34

Chapter 4: Kalman Filter 36

4.1	Introduction.....	36
4.2	Kalman Filter Design.....	37
4.3	Simulation Results	42
Chapter 5: Simulations and Experimental results		48
5.1	Simulation Results	48
5.2	Experimental Results	52
Chapter 6: Conclusions and Future Works		54
6.1	Conclusions.....	54
6.2	Future Works	55
References.....		57
Publications and Conferences.....		62
APPENDIX A		63



Controller System Design of Two Wheeled Mobile Inverted Pendulum

Chetanraj D. Patil

**Department of Interdisciplinary program of Mechatronics
Engineering,
The Graduate School, Pukyong National University**

Abstract

This thesis proposes a controller system design method using PD control and backstepping control method to stabilize and to control motion of the two wheeled mobile inverted pendulum. It also presents development results of two wheeled mobile inverted pendulum as follows: Two wheeled mobile inverted pendulum is composed of base platform and chassis with two coaxial wheels. The nonlinear dynamic modeling derived using Newton's 2nd law are presented for two wheeled mobile inverted pendulum. The derived nonlinear dynamic modeling of two wheeled mobile inverted pendulum is linearized. Based on its linearized dynamic modeling of wheel and chassis, a controller system is proposed. The proposed controller system consists of three loops composed of balance control loop, rotation control loop for chassis and position control loop for two wheeled mobile inverted pendulum. The balance and rotation control loops are designed by using Lyapunov function and

backstepping control method. The position loop is designed based on PD control method.

A control system to implement the proposed controller system is developed based on PIC 18F452 microcontroller. To obtain the information of two wheeled mobile inverted pendulum state variables, the following sensors are used: encoders, inclinometer sensor and compass sensor. The angle of two wheeled mobile inverted pendulum is measured using inclinometer. Encoders are used to measure the speed of the wheels. The compass sensor is used to measure the rotation angle. The Kalman filter is used to reduce the sensor noise and to estimate the pitch angle and moving displacement based on filtered sensor data.

The two wheeled mobile inverted pendulum is manufactured to experiment the proposed controller system. Finally, the simulation and experimental results are shown to prove effectiveness and the applicability of the proposed controller system.

Keywords: Two Wheeled Mobile Inverted Pendulum, PD Control, Backstepping Control, Kalman Filter Etc.

List of Figures

Fig. 1.1	Crane machine	2
Fig. 1.2	Segway RMP	2
Fig. 1.3	JOE: A mobile inverted pendulum	4
Fig. 2.1	Structure of two wheeled mobile inverted pendulum	10
Fig. 2.2	Configuration of control system	12
Fig. 2.3	Developed PIC-based control system	13
Fig. 2.4	Pin diagram of PIC18F452	14
Fig. 2.5	Inclinometer sensor	15
Fig. 2.6	DC motor driver	16
Fig. 2.7	Rotary encoder	17
Fig. 2.8	Compass sensor	18
Fig. 2.9	Configuration of two wheeled mobile inverted pendulum	20
Fig. 2.10	Free body diagram of two wheeled mobile inverted pendulum	22
Fig. 2.11	Free body diagram of left wheel	23
Fig. 2.12	Free body diagram of right wheel	24
Fig. 3.1	Structure of controller system	30
Fig. 4.1	Moving displacement x_r of system in simulation with/without applying Kalman filter	44
Fig. 4.2	Pitch angle θ_p in simulation with/without applying Kalman filter	45
Fig. 4.3	Yaw angle δ in simulation with/without applying Kalman filter	46
Fig. 5.1	Pitch angle θ_p in simulation result	49
Fig. 5.2	Moving displacement x_r in simulation result	50
Fig. 5.3	Yaw angle δ in simulation result	51

Fig. 5.4 Pitch angle θ_p with Kalman filter in experimental result	.52
Fig. 5.5 Moving displacement of two wheeled mobile inverted pendulum in experiment	53



List of Tables

Table 2.1 Specification of inclinometer sensor	15
Table 2.2 Specification of compass sensor	18
Table 2.3 Nomenclature of two wheeled mobile inverted pendulum	21
Table 4.1 Parameter values and initial conditions	42
Table 5.1 Numerical parameters and initial values for simulation ...	48



Chapter 1: Introduction

1.1 Motivation and Background

The inverted pendulum is a classic problem in dynamics and control theory and is widely used as a benchmark for testing control algorithms. The most fundamental one is the case that a pendulum is mounted on a cart which can move back and forth in one linear direction. The pendulum is then balanced in upright position by controlling the movement of the cart. Balancing an upturned broomstick on the end of one's finger is a simple demonstration, and the problem is solved in the technology of the Segway PT, a self-balancing transportation device. The inverted pendulum principle can be varied in many ways to make the system more complex

There are many instances of the inverted pendulum model both man-made and found in the natural world. Arguably the most prevalent example of an inverted pendulum is a human being. A person with an upright body needs to make adjustments constantly to maintain balance whether he/she is standing, walking, or running. Fig. 1.2 shows the Segway RMP. It is a device that transports one person at relatively low speed. The low-speed (limited to approximately 12 mph) operation combined with its electric propulsion system makes the Segway a candidate for providing short-distance transportation on city streets, sidewalks, and inside buildings. A crane as shown in Fig. 1.1 is a lifting machine; generally cranes are commonly employed in the transport industry for the loading and unloading of freight in the construction industry for the movement of materials and in the manufacturing industry for the assembling of heavy equipment.



Fig. 1.1 Crane machine



Fig. 1.2 Segway RMP

1.2 Literature Review

In literature, the structures of two wheeled inverted pendulum were presented in [1 ~ 4]. Li, J. [1] proposed two wheeled inverted pendulum mobile robot as a portable transporter due to its high maneuverability and small footprint. Choi, D. et al. [2] proposed human friendly motion control of a wheeled inverted pendulum by reduced order disturbance observer. Kim, Y. et al. [3] proposed that a portable transporter was suggested as a suitable unit for home and office environments of a nonholonomic two wheeled inverted pendulum robot system. Controlling such a system as two wheeled inverted pendulum is a challenging problem due to its nonlinearities, complex dynamics and uncertain environmental conditions [4].

The dynamic modeling of the two wheeled mobile inverted pendulum were proposed in following researches. Ko, A. et al. [5] proposed that modeling of the self balancing robot is complex because of the rolling/slipping constraints of the wheels. In spite of its dynamic complexity, numerous two-wheeled inverted pendulums have been created by research institutions and companies. In 1988, Kawamura, T. et al. [6] modeled the coaxial bicycle as an inverted pendulum pivoted on wheel axis. Ha, Y. S. et al. [7] developed an autonomous two wheeled inverted pendulum robot. This robot was modeled by two independent driving wheels on the same axle and its vertical axis. Huang, J. et al. [8] proposed a mobile wheeled inverted pendulum. Dynamic modeling of the mobile wheeled inverted pendulum is based on Lagrange formula. In 2000, Ding, F. et al. [9] designed a two wheeled inverted pendulum platform to act as a personal transporter. Dynamic modeling of the system was proposed

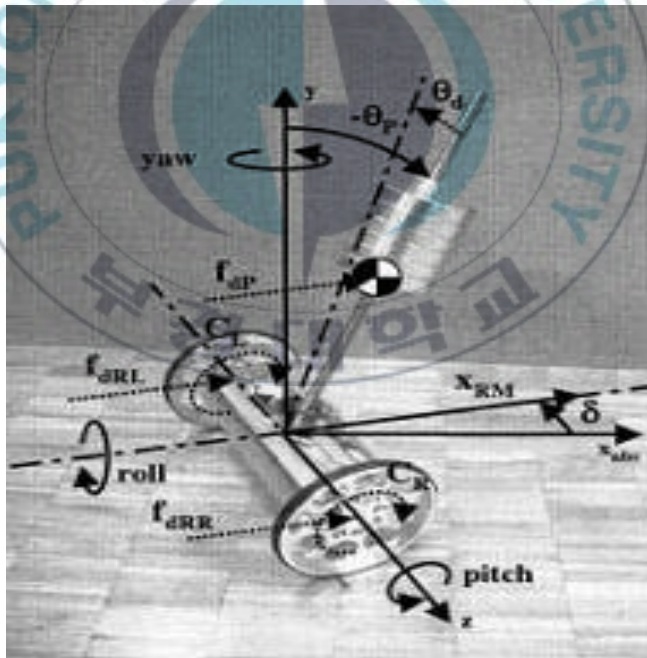


Fig. 1.3 JOE: A mobile inverted pendulum

The unmodeled dynamics of two wheeled mobile inverted pendulum have motivated researchers to explore model-free control

techniques such as neural networks and fuzzy logic implementations. However, other researchers have tried to understand these dynamics and design control techniques. For instance, in 2007, Jung, S. et al. [20] combined a neural network with a PID control to perform balancing and path following tasks for wheel driven mobile inverted pendulum, but more uncertainties are presented in the mobile pendulum system since rolling on the floor causes inconsistent disturbance to the system due to irregular surface of the floor. In 2009, Li, Z. et al. [21] implemented an adaptive fuzzy controller to wheeled inverted pendulum with parametric and functional uncertainties. Vlassis, N. et al. [22] applied a Monte Carlo expectation-maximization algorithm to self balancing robot to achieve balance by model free reinforcement learning. In 2011, a fuzzy logic controller was designed by Huang, C. et al. [23] to achieve stabilization and velocity control for a self balancing transporter system. In 2010, Li, Z. et al. [25] proposed a wheeled inverted pendulum system considering the friction between the wheels and the driving surface as uncertainties, and tested an adaptive fuzzy control on this model.

Several control approaches have been used to stabilize two-wheeled inverted pendulum. Pathak, K. et al. [17] used partial feedback linearization to design a two level position stabilization control and velocity control of wheeled inverted pendulum system. Nawawi, S. et al. [18] used a pole-placement control strategy to stabilize a two wheeled inverted pendulum robot. In 2007, Jeong, S. H. et al. [19] implemented a LQR state feedback control for their mobile humanoid experimental robot. In 2003, Bui, T. H. et al. [24] developed a two wheeled welding mobile robot consisting of a welding torch mounted on a two-wheeled inverted pendulum that was

able to follow a specified welding trajectory using simple nonlinear controller.

In sliding mode control method of two wheeled inverted pendulum, several research results have been implemented [9, 16, 28]. In the year 2000, Ding, F. et al. [9] used a terminal sliding mode control method and applied it to control the novel narrow vehicle. Kang, M. T. et al. [16] used sliding mode technique to control a mobile inverted pendulum. Choi, N. S. et al. [28] designed sliding mode controller to stabilize the inverted pendulum at upright position under straight line motion against disturbance of mobile inverted pendulum.

Backstepping control methods have been used to stabilize two wheeled mobile inverted pendulum. For instance, Thao, N. G. M. et al. [26] proposed a PID backstepping controller for two wheeled self-balancing robot to keep the motion of robot to track a reference signal. Altoniz, O. T. [29] proposed adaptive integral backstepping control method for motion control of inverted pendulum with unknown parameters of total effective inertia and acting torque of wheels by using the general motion control model. Benaskeur, A. et al. [15] proposed an adaptive backstepping controller used to stabilize the inverted pendulum with the unknown parameter of one-half of the length of the rod. Ruan, X. et al. [30] proposed fuzzy backstepping controller for two wheeled self balancing robot.

However, the two wheeled mobile inverted pendulum provides some problems from its structure. For example, it is difficult to derive modeling of two wheeled mobile inverted pendulum, especially dynamic modeling. Therefore, obtaining the dynamic modeling and

motion control of two wheeled mobile inverted pendulum are very deeply needed.

1.3 Objective and Researching Method

The objective of this thesis is to present modeling and innovative control algorithms to stabilize and control the motion of two wheeled mobile inverted pendulum system. To do this, the following tasks are done. Firstly, hardware configuration and dynamic modeling of two wheeled mobile inverted pendulum based on Newton's 2nd law is proposed. Secondly, based on the linearized dynamic modeling, a controller system is proposed. It consists of three loops composed of balance control, rotation control and position control loop. The balance and position control loops are designed by using Lyapunov function and backstepping control method. The position control loop is designed by PD control method. Finally, the Kalman filter is proposed to reduce sensor noise and to estimate the pitch angle and moving displacement based on filtered sensor data. To implement the proposed controller system, a control system is developed based on PIC18F452, encoders, inclinometer sensor and compass sensor. Simulation and experimental results show that the two wheeled mobile inverted pendulum system are successfully controlled by proposed controller system. Therefore, the simulation and experimental results shows the effectiveness and applicability of the proposed controller system for the two wheeled mobile inverted pendulum system.

1.4 Outline of thesis and summary of contributions

This thesis consists of six chapters. The content and summary of contributions in each chapter are summarized as follows:

➤ Chapter 1: Introduction

Background and motivation, objective and researching method and the outline and summary of contributions of this thesis are presented.

➤ Chapter 2: System Description and System Modeling

In this chapter, System description and dynamic modeling of two wheeled mobile inverted pendulum are proposed. The dynamic modeling of wheels and chassis of two wheeled mobile inverted pendulum are introduced based on Newton's 2nd law. The linearized dynamic modeling of the system is proposed. This chapter also describes the structure of hardware system of two wheeled mobile inverted pendulum including inclinometer sensor, encoder and compass sensor. The inclinometer sensor is used to measure the pitch angle of chassis and compass sensor is used to measure the rotation angle of two wheeled mobile inverted pendulum. Two encoders are used to measure the motor speed. A control system is developed based on microcontroller PIC18F452 to implement the presented controller system.

➤ **Chapter 3: Controller System Design**

In this chapter, a controller system of the two wheeled mobile inverted pendulum using PD control and backstepping control methods is proposed based on its linearized modeling. The controller system consists of three loops such as balance control loop, rotational control loop and position control loop. The balance and rotation control loops are designed by using Lyapunov function and backstepping method. The position control loop is designed based on PD control method.

➤ **Chapter 4: Kalman filter**

In this chapter, a Kalman filter algorithm is proposed for estimating the moving displacement of two wheeled mobile inverted pendulum and pitch angle with sensor noise. To verify the effectiveness of Kalman filter, simulation and experiment are done.

➤ **Chapter 5: Simulation and Experimental Results**

The simulation and experimental results are shown to prove the effectiveness and the applicability of the proposed modeling and the proposed controller system.

➤ **Chapter 6: Conclusion and Future works**

Some conclusions of this thesis and future works are presented.

Chapter 2: System Description and System Modeling

2.1 System Description

This describes the hardware structure of the two wheeled mobile inverted pendulum system including encoders, sensors and hardware configuration of control system developed to implement the designed controller system. Fig. 2.1 shows the structure of two wheeled mobile inverted pendulum system used for this thesis.

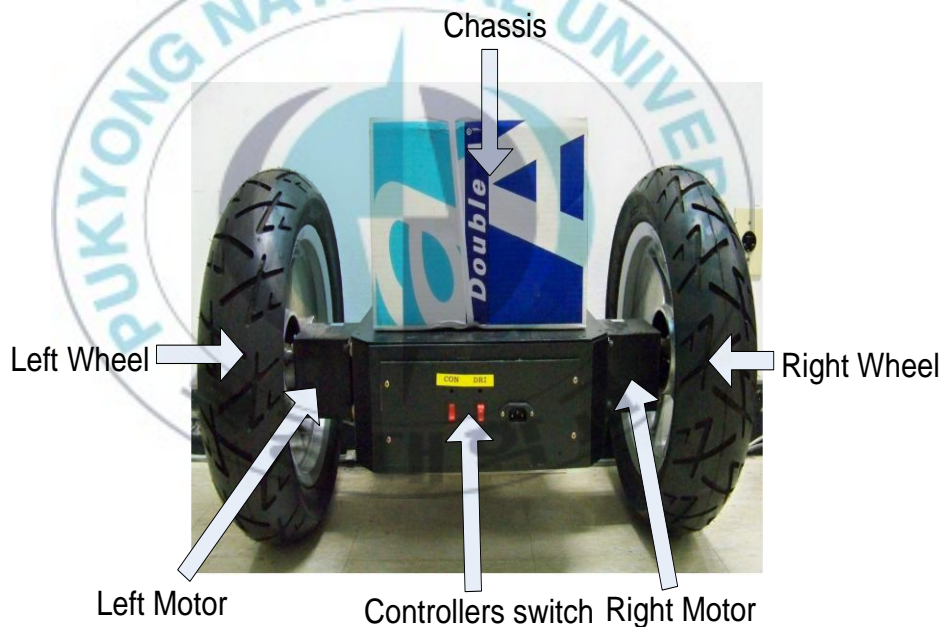


Fig. 2.1 Structure of two wheeled mobile inverted pendulum system.

For implementing the designed controller system, a PIC-based control system was developed. The developed control system is composed of three parts: two slave microcontrollers and one master microcontroller. The configuration diagram of overall control system is shown in Fig. 2.2. In the diagram, two slave PIC18F452 microcontrollers are integrated into one module for controlling two motors of the left wheel and the right wheel, respectively. The motors are driven via KDC248H H-bridge motor drivers. One PIC18F452 microcontroller is used as master, and receives the signals from sensors. The slave controllers are responsible for controlling the motor speed. The master microcontroller communicates to motors drivers via I2C and all three microcontrollers are communicates to the host computer via RS232 interface. The configuration for sensors is developed to obtain system states and realize the above controllers, including an inclinometer sensor, compass sensor and two encoders. The compass sensor is used to measure the angle of rotation of two wheeled mobile inverted pendulum. An inclinometer sensor is used to measure the pitch angle of chassis. An incremental encoders are utilized to measure the speed of the wheels. The implementation of PIC-based control system including two slave microcontrollers and one master controller as shown in Fig. 2.3

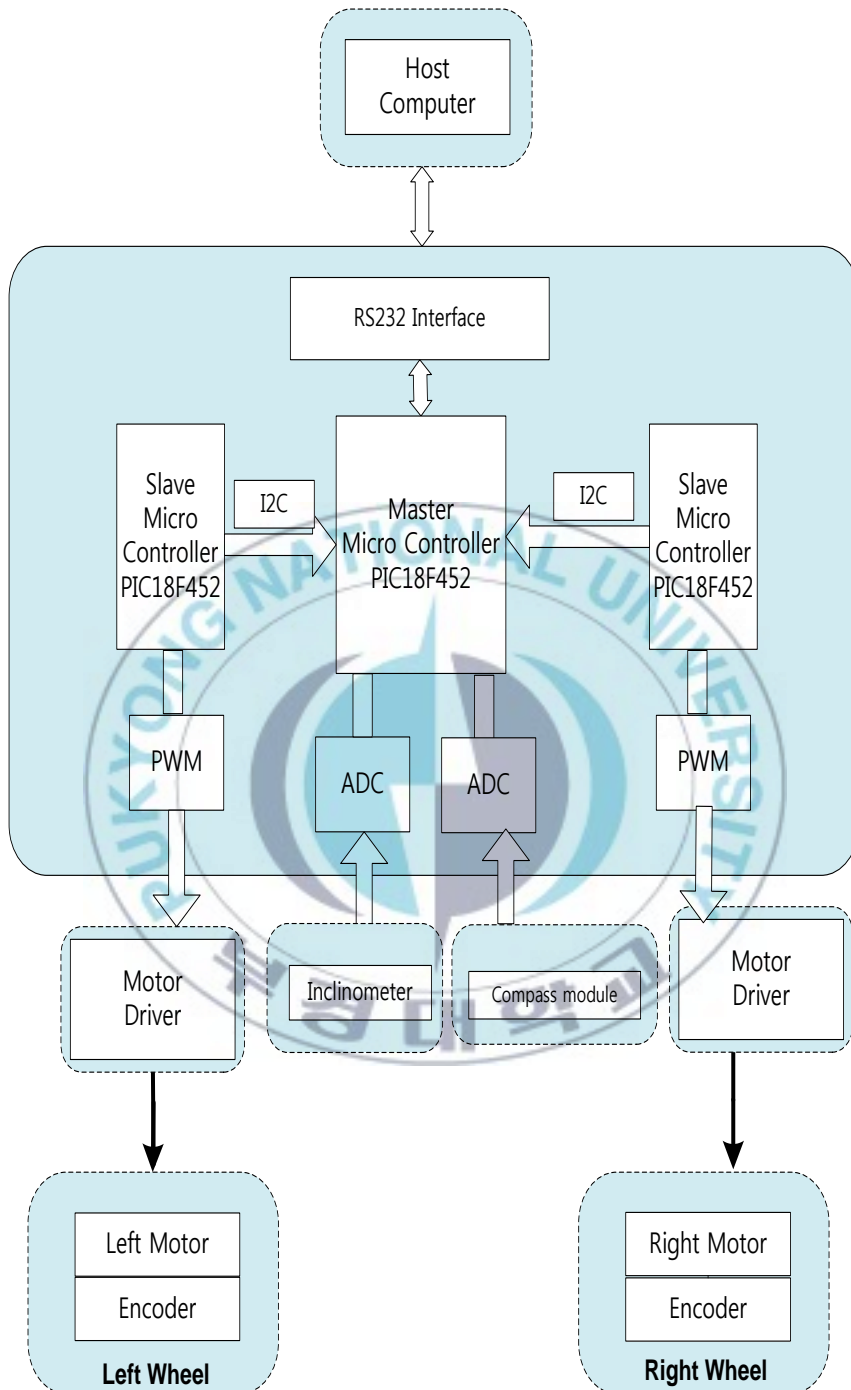


Fig. 2.2 Configuration of control system

➤ **Developed PIC-based control system:**

Fig. 2.3 shows the developed PIC-based control system. There are three PIC18F452 microcontrollers that are integrated into one module. One PIC18F452 is used as master, and receives the signals from sensors and other two PIC18F452 microcontrollers are used for controlling two motors of the left and right wheels. The master communicates to the motor drivers via I2C

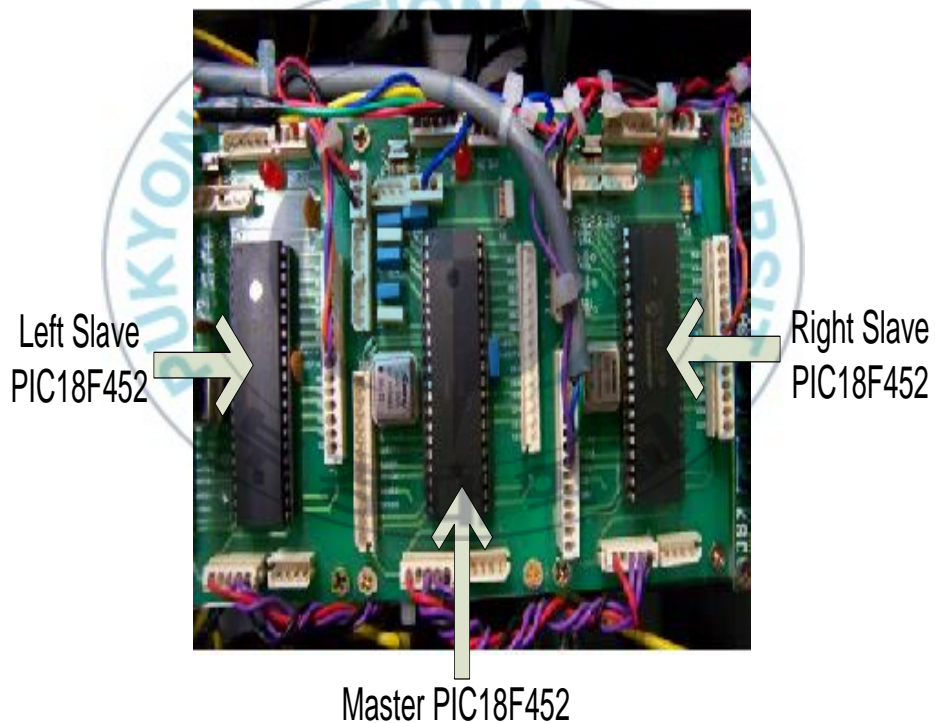


Fig. 2.3 Developed PIC-based control system.

➤ **PIC18F452 Microcontroller:**

The PIC18F452 is a 40 pin, high performance microcontroller in Fig. 2.4. The main specifications are summarized as follows:

- On chip program memory (FLASH): 32K (bytes)
- Data memory (RAM): 1536 (bytes)
- EEPROM data memory: 256 (bytes)
- Interrupts: 18 sources
- Timer: 4
- Two Capture/Compare/PWM modules
- 10 bit analog to digital module: 8 input channels
- Serial Communications: Master Synchronous Serial Port (MSSP) operates in two modes, Serial Peripheral Interface (SPI) and I2C (master/slave).
- Power saving SLEEP mode

With the functions on PIC18F452 above, its pin diagram is shown in Fig. 2.4.

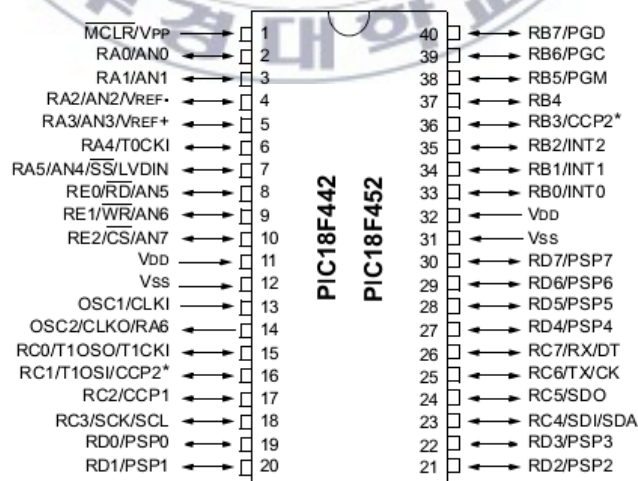


Fig. 2.4 Pin diagram of PIC18F452

➤ **Inclinometer Sensor:**

Fig. 2.5 shows the inclinometer sensor used in two wheeled mobile inverted pendulum system. An inclinometer is an instrument for measuring angles of tilt or elevation of an object with respect to gravity. Electronic inclinometer can achieve output resolution 0.0001 degrees depending on the technology and angle range that may be limited to 0.01 degree.

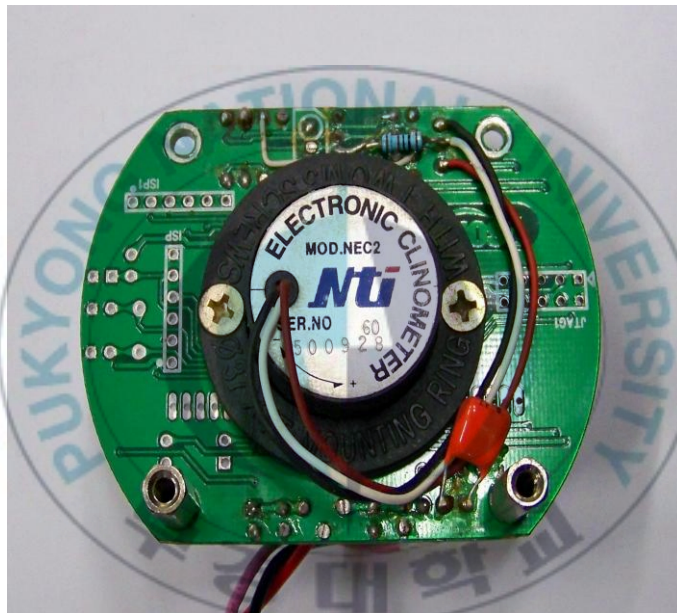


Fig. 2.5 Inclinometer sensor

Table 2.1 Specification of inclinometer sensor

Specification	Range
Voltage Supply	DC 12V
Output voltage	0 ~ 10V
Measurement range	-60° ~ 60°

➤ DC Motors:

The two wheeled mobile inverted pendulum has two wheels. The wheels are directly driven by two 300W DC motors.

Each DC motor using 24V DC power supplier is driven by each motor driver as shown in Fig. 2.6. Maximum current allowed by the driver is up to 250 A with 24V DC.

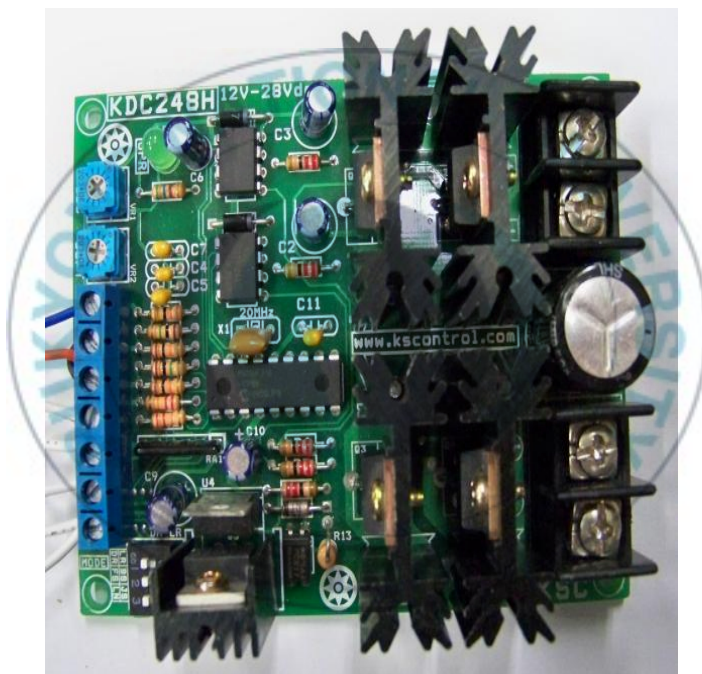


Fig. 2.6 DC motor driver

➤ **Rotary Encoder:**

Fig. 2.7 shows rotary encoder that converts the angular position or motion of shaft or axle to an analog or digital signal. The encoder as shown in the Fig. 2.7 is incremental encoder. The output of an incremental encoder provides information about the motion of shaft which is typically further processed elsewhere into information such as speed, distance and position.



Fig. 2.7 Rotary encoder

➤ Compass Sensor:

The CMPS03 compass module has been specifically used to measure the rotation angle of two wheeled mobile inverted pendulum. Fig.2.8 shows description of compass sensor and Table 2.2 shows specification of compass sensor.

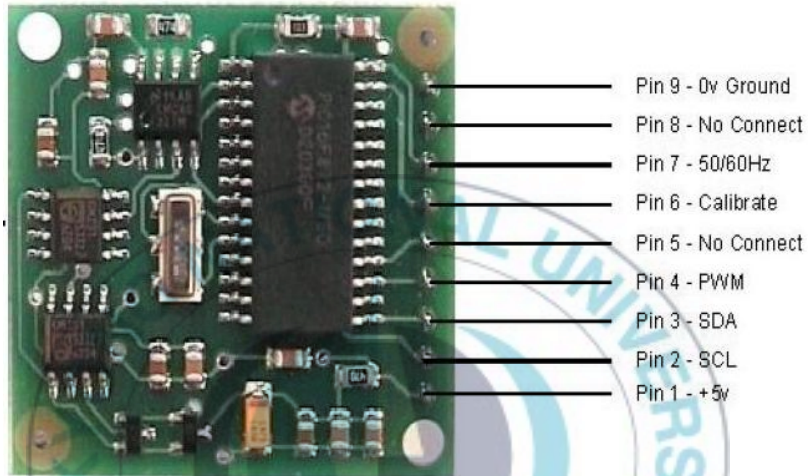


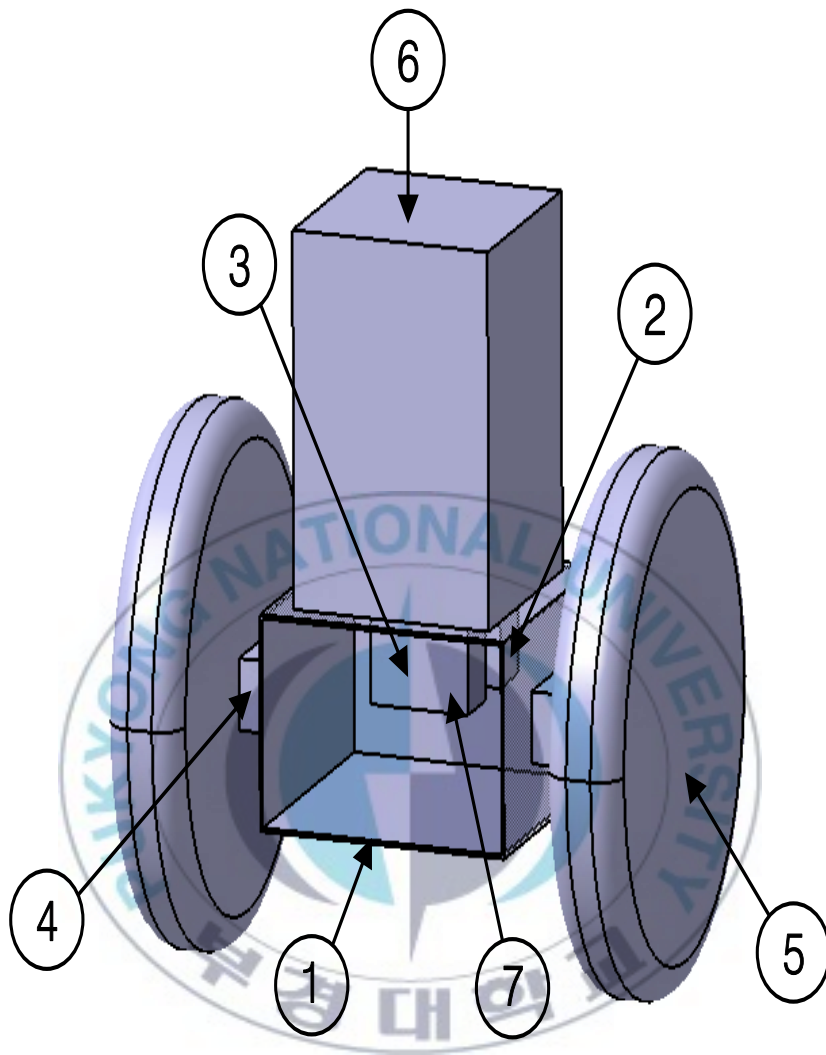
Fig. 2.8 Compass sensor

Table 2.2 Specification of compass sensor

Specification	Range
Voltage Supply	5V
Current	25mA
Resolution	0.1°
Accuracy	3° ~ 4° approx. after calibration
Output	I2C Interface, SMBUS compatible, 0 ~ 255 and 0 ~ 3599
SCL speed	up to 1MHz
Small Size	32mm x 35mm

2.2 System Modeling

This presents dynamic modeling of two wheeled mobile inverted pendulum system. To form a two-wheeled mobile inverted pendulum, the chassis ⑥ is anchored to a base platform ① that has a wheel ⑤ mounted on each side as shown in Fig. 2.9. In this case, motor ④ drives each wheel independently. Two encoders ④ are used to measure the motor speed. The torque from the motors makes the base platform move to balance pitch angle of the pendulum as shown in Fig. 2.10. System consists of inclinometer sensor ③ used to detect the pitch angle of two wheeled mobile inverted pendulum. PIC18F452 microcontrollers ② are used to control the two wheeled mobile inverted pendulum. Compass sensor ⑦ is used to detect rotation angle of the two wheeled mobile inverted pendulum. The nomenclature of the two wheeled mobile inverted pendulum is shown in Table 2.3



① Base Platform	② Microcontroller
③ Inclinometer sensor	④ Motor & Encoder
⑤ Wheel	⑥ Chassis
⑦ Compass sensor	

Fig. 2.9 Configuration of two wheeled mobile inverted pendulum

Table 2.3 Nomenclature of two wheeled mobile inverted pendulum

Parameters	Description	Units
θ_p	Pitch angle	[degree]
δ	Yaw angle	[degree]
x_r	Moving displacement of two wheeled mobile inverted pendulum	[m]
$J_{RL} = J_{RR} = J_r$	Moment of inertia of the wheel	[kgm ²]
$M_{RL} = M_{RR} = M_r$	Mass of the wheel	[kg]
J_p	Moment of inertia of the inverted pendulum with respect to the z axis	[kgm ²]
J_δ	Moment of inertia of the inverted pendulum with respect to the y axis	[kgm ²]
M_p	Mass of the inverted pendulum	[kg]
R	Radius of wheel	[m]
L	Distance between the wheel's center and the pendulum's center of gravity	[m]
D	Distance between the wheels	[m]
x_p, y_p	Position of the pendulum with respect to the x axis and y axis, respectively.	[m]
g	Gravitational acceleration	[m / s ²]
τ_L, τ_R	Input torque for left and right wheels	[Nm]
x_{RL}, x_{RR} y_{RL}, y_{RR}	Position of the left and right wheels with respect to x axis and y axis, respectively	[m]
H_L, H_R V_L, V_R	Reaction forces between left/right wheels and pendulum	[N]
H_{TL}, H_{TR} V_{TL}, V_{TR}	Reaction forces between left/right wheels and ground	[N]
θ_{RL}, θ_{RR}	Rotational angle of left and right wheels	[degree]
f_{dRL}, f_{dRR}	Disturbance forces to the center of the left/right wheels	[N]
$f_{dP}, F_{C\theta}$	Horizontal and vertical disturbance forces to the center gravity of the pendulum	[N]
(x, y, z)	Main coordinates of the system	
(x_{abs}, y, z_{abs})	Absolute coordinates of the system	

Fig. 2.10 shows the free body diagram about the motion of two wheeled mobile inverted pendulum

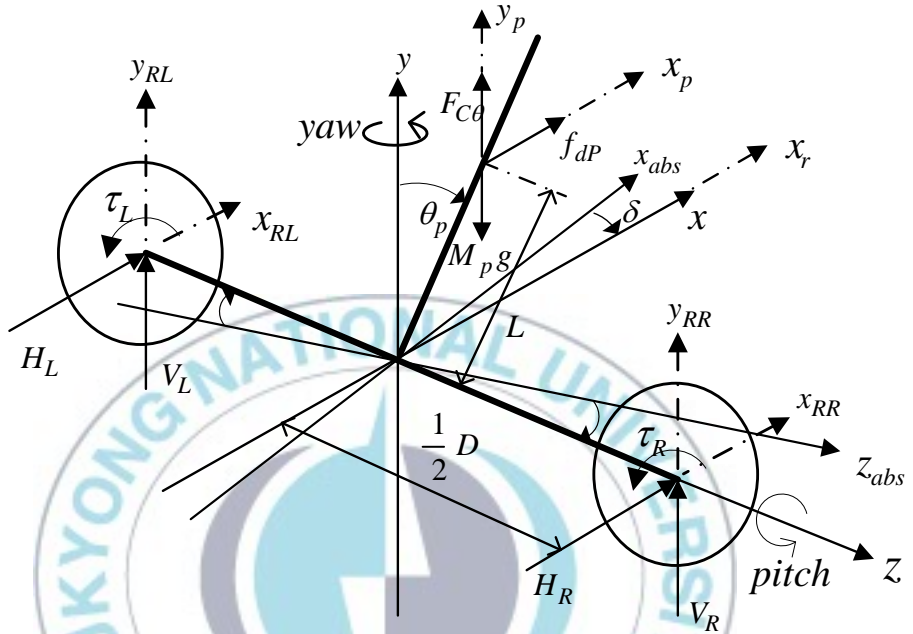


Fig. 2.10 Free body diagram of two wheeled mobile inverted pendulum

2.2.1 Characterization of Wheels

This section describes for wheel dynamics. The equations for the left wheel are presented.

To develop this system, it is assumed that

- Both wheels have same radius.
- Both wheels have same mass.
- The wheels are not deformable.

- The wheels are rotated with no slipping and pure rolling.

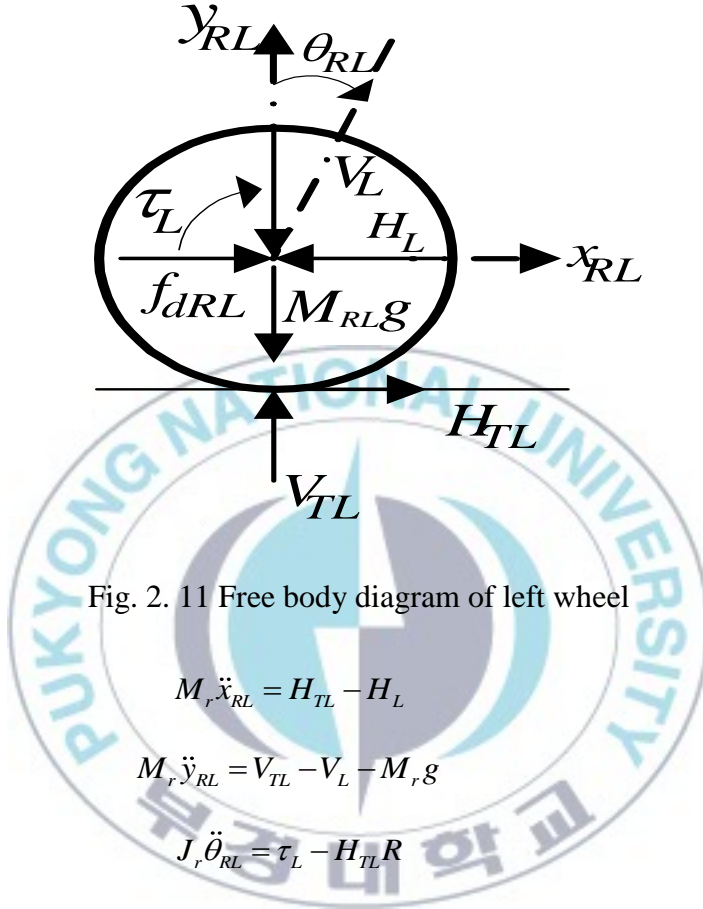


Fig. 2. 11 Free body diagram of left wheel

$$M_r \ddot{x}_{RL} = H_{TL} - H_L \quad (2.1)$$

$$M_r \ddot{y}_{RL} = V_{TL} - V_L - M_r g \quad (2.2)$$

$$J_r \ddot{\theta}_{RL} = \tau_L - H_{TL} R \quad (2.3)$$

where $M_{RL} = M_r$; $J_{RL} = J_r$

Since linear motion is acting on center of wheel, a transformation from angular rotation into linear motion can be made as follows:

$$\dot{x}_{RL} = R \dot{\theta}_{RL} \rightarrow \ddot{x}_{RL} = R \ddot{\theta}_{RL} \rightarrow \ddot{\theta}_{RL} = \frac{\ddot{x}_{RL}}{R} \quad (2.4)$$

From Eqs. (2.3) and (2.4), horizontal reaction force is expressed as:

$$H_{TL} = \frac{\tau_L}{R} - \frac{J_r}{R^2} \ddot{x}_{RL} \quad (2.5)$$

By substituting Eq. (2.5) into Eq. (2.1), the following is obtained.

$$\left(M_r R + \frac{J_r}{R} \right) \ddot{x}_{RL} = \tau_L - H_L R \quad (2.6)$$

Now the equations for the right wheel are presented as follows:

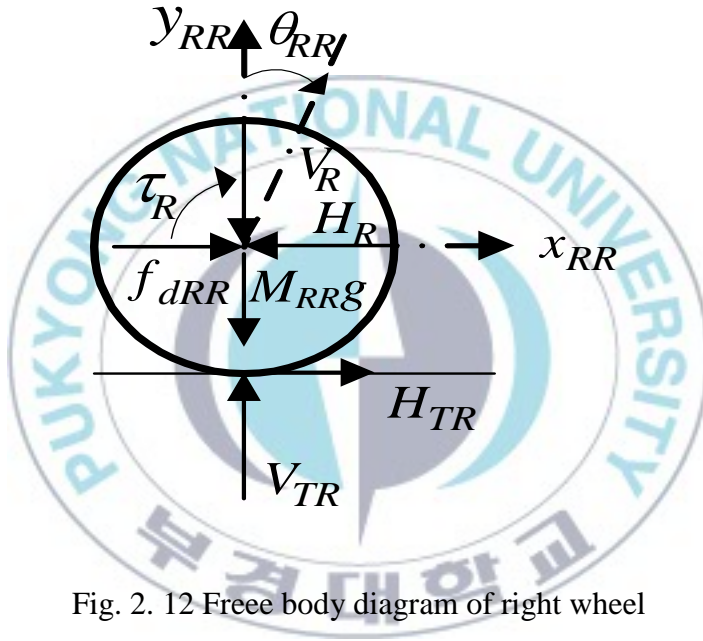


Fig. 2. 12 Free body diagram of right wheel

$$M_r \ddot{x}_{RR} = H_{TR} - H_R \quad (2.7)$$

$$M_r \ddot{y}_{RR} = V_{TR} - V_R - M_r g \quad (2.8)$$

$$J_r \ddot{\theta}_{RR} = \tau_R - H_{TR} R \quad (2.9)$$

where $M_{RR} = M_r$; $J_{RR} = J_r$

Assuming the above conditions, the following is obtained.

$$\dot{x}_{RR} = R\dot{\theta}_{RR} \rightarrow \ddot{x}_{RR} = R\ddot{\theta}_{RR} \rightarrow \ddot{\theta}_{RR} = \frac{\ddot{x}_{RR}}{R} \quad (2.10)$$

From Eqs. (2.9) and (2.10), horizontal reaction force is obtained as:

$$H_{TR} = \frac{\tau_R}{R} - \frac{J_r}{R^2} \ddot{x}_{RR} \quad (2.11)$$

By substituting Eq. (2.11) into Eq. (2.7), the following is obtained.

$$\left(M_r R + \frac{J_r}{R} \right) \ddot{x}_{RR} = \tau_R - H_R R \quad (2.12)$$

2.2.2 Body Dynamics

The coordinates of two wheeled mobile inverted pendulum is given as follows:

$$x_p = L \sin \theta_p + x_r \quad (2.13)$$

$$y_p = L \cos \theta_p \quad (2.14)$$

where x_r is moving displacement of two wheeled mobile inverted pendulum.

$$x_r = \frac{x_{RL} + x_{RR}}{2} \quad (2.15)$$

Applying the Newton's 2nd law to the chassis, the following equations are obtained.

$$M_p \ddot{x}_p = H_L + H_R \quad (2.16)$$

$$M_p \ddot{y}_p = V_L + V_R - M_p g \quad (2.17)$$

Taking moment about the center of gravity yields the torque equation as follows:

$$J_p \ddot{\theta}_p = (V_L + V_R) L \sin \theta_p - (H_L + H_R) L \cos \theta_p \quad (2.18)$$

From Eqs. (2.6) ~ (2.18), the dynamic equation of two wheeled mobile inverted pendulum is given as follows:

$$\left(2M_r R + \frac{2J_r}{R} + M_p R \right) \ddot{x}_r + M_p R L (\ddot{\theta}_p \cos \theta_p - \dot{\theta}_p^2 \sin \theta_p) = \tau_L + \tau_R \quad (2.19)$$

$$(J_p + M_p L^2) \ddot{\theta}_p - M_p g L \sin \theta_p + M_p L \cos \theta_p \ddot{x}_r = 0 \quad (2.20)$$

The moment of the two wheeled mobile inverted pendulum with respect to y axis is given by:

$$J_\delta \ddot{\delta} = (H_L - H_R) \frac{D}{2} \quad (2.21)$$

When two wheeled mobile inverted pendulum turns right as an angle δ , linear velocities of left and right wheels with respect to x axis are as follows:

$$\dot{x}_{RL} = \dot{x}_r + \left(\frac{\dot{\delta} D}{2} \right) \quad (2.22)$$

$$\dot{x}_{RR} = \dot{x}_r - \left(\frac{\dot{\delta} D}{2} \right) \quad (2.23)$$

From Eqs. (2.22) ~ (2.23), the following is obtained.

$$\dot{\delta} D = \dot{x}_{RL} - \dot{x}_{RR} \quad (2.24)$$

The time derivative of Eq. (2.24) is obtained as follow:

$$\ddot{\delta}D = \ddot{x}_{RL} - \ddot{x}_{RR} \quad (2.25)$$

From Eq. (2.6), Eq. (2.12), Eq. (2.21) and Eq. (2.25) the following is obtained.

$$\left[\frac{2J_{\delta}R}{D} + \left(\frac{M_r R^2 + J_r}{R} \right) D \right] \ddot{\delta} = \tau_L - \tau_R \quad (2.26)$$

From Eqs. (2.19) ~ (2.20) and Eq. (2.26), the dynamic equations of two wheeled mobile inverted pendulum are described as follows:

$$\begin{aligned} (M_p RL \cos \theta_p - \phi_1 \phi_2 \sec \theta_p) \ddot{\theta}_p + \phi_1 g \tan \theta_p \\ - M_p RL \dot{\theta}_p^2 \sin \theta_p = \tau_L + \tau_R \end{aligned} \quad (2.27)$$

$$\cos \theta_p \ddot{x}_r = g \sin \theta_p - \phi_2 \ddot{\theta}_p \quad (2.28)$$

$$\phi_3 \ddot{\delta} = \tau_L - \tau_R \quad (2.29)$$

where

$$\begin{cases} \phi_1 = 2M_r R + \frac{2J_r}{R} + M_p R \\ \phi_2 = \frac{(J_p + M_p L^2)}{M_p L} \\ \phi_3 = \frac{2J_{\delta}R}{D} + \left(\frac{M_r R^2 + J_r}{R} \right) D \end{cases} \quad (2.30)$$

Assuming the small change of pitch angle θ_p gives $\sin \theta_p \cong \theta_p$, $\cos \theta_p \cong 1$ and $\dot{\theta}_p^2 \cong 0$ for linearizing Eqs. (2.27) ~ (2.29).

This leads the dynamics Eqs. (2.27) ~ (2.29) to the following linearized equation of motion.

$$(M_p RL - \phi_1 \phi_2) \ddot{\theta}_p + \phi_1 g \theta_p = \tau_L + \tau_R \quad (2.31)$$

$$\ddot{x}_r = g \theta_p - \phi_2 \ddot{\theta}_p \quad (2.32)$$

$$\phi_3 \ddot{\delta} = \tau_L - \tau_R \quad (2.33)$$

Eqs. (2.31) ~ (2.33) represents the system in state space form.

$$\dot{x} = Ax + Bu \quad (2.34)$$

$$y = Cx \quad (2.35)$$

where x is a system state variable vector, y is an output variable vector, u is an input variable vector and A , B , and C are matrices as follows:

$$A = \begin{bmatrix} 0 & 1 & 0 & 0 & 0 & 0 \\ 0 & 0 & A_{23} & 0 & 0 & 0 \\ 0 & 0 & 0 & 1 & 0 & 0 \\ 0 & 0 & A_{43} & 0 & 0 & 0 \\ 0 & 0 & 0 & 0 & 0 & 1 \\ 0 & 0 & 0 & 0 & 0 & 0 \end{bmatrix} \quad (2.36)$$

$$B = \begin{bmatrix} 0 & 0 \\ B_{21} & 0 \\ 0 & 0 \\ B_{41} & 0 \\ 0 & 0 \\ 0 & B_{62} \end{bmatrix} \quad (2.37)$$

$$C = \begin{bmatrix} 1 & 0 & 0 & 0 & 0 & 0 \\ 0 & 0 & 1 & 0 & 0 & 0 \\ 0 & 0 & 0 & 0 & 1 & 0 \end{bmatrix} \quad (2.38)$$

$$x = [x_r \ \dot{x}_r \ \theta_p \ \dot{\theta}_p \ \delta \ \dot{\delta}]^T \quad (2.39)$$

$$u = [u_1 \ u_2]^T = [\tau_L + \tau_R \quad \tau_L - \tau_R]^T \quad (2.40)$$

$$y = [y_1 \ y_2 \ y_3]^T \quad (2.41)$$

with

$$A_{23} = g + \frac{\phi_1 \phi_2 g}{M_p RL - \phi_1 \phi_2} \quad (2.42)$$

$$A_{43} = \frac{-\phi_1 g}{M_p RL - \phi_1 \phi_2} \quad (2.43)$$

$$B_{21} = \frac{-\phi_2}{M_p RL - \phi_1 \phi_2} \quad (2.44)$$

$$B_{41} = \frac{1}{M_p RL - \phi_1 \phi_2} \quad (2.45)$$

$$B_{62} = \frac{1}{\phi_3} \quad (2.46)$$



Chapter 3: Controller System Design

This chapter designs a controller system that integrates three control loops, composed of balance control loop, rotation control loop for chassis and position control loop for two wheeled mobile inverted pendulum. The balance and rotation control loops are designed by using Lyapunov function and backstepping control method. The position control loop is designed based on PD control method. Fig. 3.1 shows the structure of controller system.

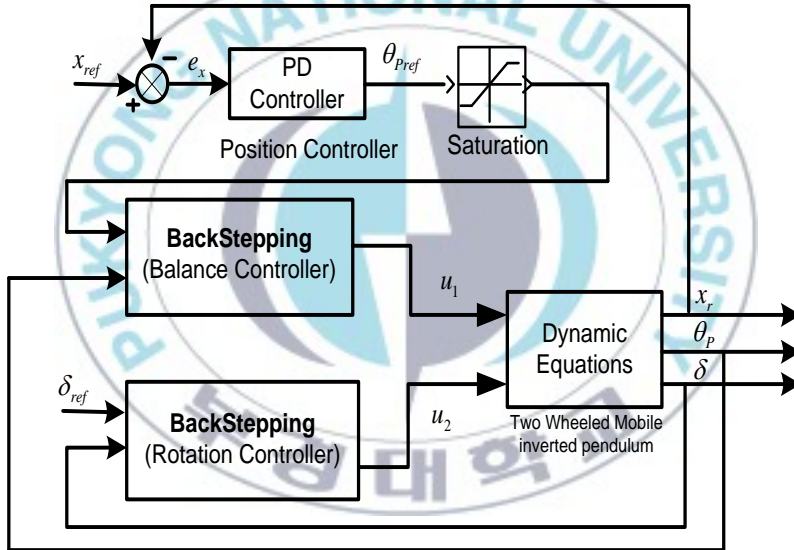


Fig. 3.1 Structure of controller system

3.1 Backstepping Controller Design

The backstepping controller design method for two wheeled mobile inverted pendulum's balance is proposed as follows:

3.1.1 Balance Controller Design

Defining $x_3 = \theta_p$ and $x_4 = \dot{\theta}_p$, Eqs. (2.31) ~ (2.33) are rewritten as follows:

$$g(x_3)\dot{x}_4 + h(x_3) = u_1 \quad (3.1)$$

$$h(x_3) = \phi_1 g x_3 \quad (3.2)$$

$$g(x_3) = M_p RL - \phi_1 \phi_2 \quad (3.3)$$

where $u_1 = \tau_1 + \tau_2$ is first control input,

Using Eqs. (2.30) and (3.3), the following condition is obtained;

$$0 < M_p RL < \phi_1 \phi_2 \quad (3.4)$$

Because $g(x_3) \neq 0$ from Eqs. (3.3) and (3.4), Eq. (3.1) yields:

$$\dot{x}_4 = \frac{u_1 - h(x_3)}{g(x_3)} \quad (3.5)$$

A tracking pitch angle error of the chassis is defined as follows:

$$e_1 = x_3 - x_{3ref} \quad (3.6)$$

where $x_{3ref} = \theta_{pref}$ is the reference value for θ_p

A virtual control x_{4*} is defined as:

$$x_{4*} = -k_1 e_1 + \dot{x}_{3ref} \quad (3.7)$$

And angular velocity error between the virtual control x_{4*} and x_4 as follows:

$$e_2 = x_4 - x_{4*} \quad (3.8)$$

The derivation of e_1 and e_2 can be given as follows:

$$\dot{e}_1 = \dot{x}_3 - \dot{x}_{3ref} = x_4 - \dot{x}_{4ref} = e_2 - k_1 e_1 \quad (3.9)$$

$$\dot{e}_2 = \dot{x}_4 - \dot{x}_{4*} = \dot{x}_4 + k_1 \dot{e}_1 - \ddot{x}_{3ref} \quad (3.10)$$

Substituting Eq. (3.9) into Eq. (3.10), the following can be obtained:

$$\dot{e}_2 = \dot{x}_4 + k_1 e_2 - k_1^2 e_1 - \ddot{x}_{3ref} \quad (3.11)$$

For designing balance control input, Lyapunov function is defined as follows:

$$V_1 = \frac{1}{2} e_1^2 + \frac{1}{2} e_2^2 \quad (3.12)$$

The derivative of V_1 is as follows:

$$\begin{aligned} \dot{V}_1 &= e_1 \dot{e}_1 + e_2 \dot{e}_2 \\ &= e_1 (e_2 - k_1 e_1) + e_2 (\dot{x}_4 + k_1 e_2 - k_1^2 e_1 - \ddot{x}_{3ref}) \\ &= -k_1 e_1^2 - k_2 e_2^2 \\ &\quad + e_2 \left[\frac{u_1 - h(x_3)}{g(x_3)} + (k_1 + k_2) e_2 + (1 - k_1^2) e_1 - \ddot{x}_{3ref} \right] \end{aligned} \quad (3.13)$$

To make \dot{V}_1 negative, the first control input is chosen as follows:

$$u_1 = h(x_3) + g(x_3) \left[\ddot{x}_{3ref} - (k_1 + k_2) e_2 - (1 - k_1^2) e_1 \right] \quad (3.14)$$

Substituting Eq. (3.14) to (3.13), the derivative of Lyapunov function is given by:

$$\dot{V}_1 = -k_1 e_1^2 - k_2 e_2^2 \leq 0 \quad (3.15)$$

3.1.2 Rotation Controller Design

Similarly, the procedure of backstepping controller design for two wheeled mobile inverted pendulum's rotation is as follows:

Defining $x_5 = \delta$ and $x_6 = \dot{\delta}$, Eq. (2.33) is rewritten as follows:

$$\phi_3 \dot{x}_6 = u_2 \quad (3.16)$$

where $u_2 = \tau_L - \tau_R$

Tracking yaw angle error and tracking yaw angular velocity error are defined, respectively, as follows:

$$e_3 = x_5 - x_{5ref} \quad (3.17)$$

$$e_4 = x_6 - x_{6*} \quad (3.18)$$

where $x_{5ref} = \delta_{ref}$ is the reference angle of yaw angle x_5 and the virtual control x_{6*} is chosen as follows:

$$x_{6*} = -k_3 e_3 + \dot{x}_{5ref} \quad (3.19)$$

When the two wheeled mobile inverted pendulum doesn't move, or moves forward, or moves backward (doesn't turn left-right), the reference yaw angle equals zero ($\delta_{ref} = 0$).

For designing rotation control input, Lyapunov function is defined as follows:

$$V_2 = \frac{1}{2}e_3^2 + \frac{1}{2}e_4^2 \quad (3.20)$$

The derivative of V_2 is as follows:

$$\begin{aligned} \dot{V}_2 &= e_3\dot{e}_3 + e_4\dot{e}_4 \\ &= -k_3e_1^2 - k_4e_2^2 \\ &\quad + e_2 \left[\frac{u_1}{\phi_3} + (k_3 + k_4)e_4 + (1 - k_3^2)e_3 - \ddot{x}_{5ref} \right] \end{aligned} \quad (3.21)$$

To make \dot{V}_2 negative, the second control input is as follows:

$$u_2 = \phi_3 \left[\ddot{x}_{5ref} - (k_3 + k_4)e_4 - (1 - k_3^2)e_3 \right] \quad (3.22)$$

Substituting Eq. (3.22) into Eq. (3.21), \dot{V}_2 is given by:

$$\dot{V}_2 = -k_3e_1^2 - k_4e_2^2 \leq 0 \quad (3.23)$$

3.2 PD Controller Design

3.2.1 Position Controller Design

Control system development is an imperative process to guarantee the success of stabilizing the two wheeled mobile inverted pendulum, while there is a variety of control techniques that can be applied to stabilize the two wheeled mobile inverted pendulum, the main objective of the proposed controller system is to control the system effectively.

The method for controlling the two wheeled mobile inverted pendulum will be a linear controller. A Proportional and Derivative

control method has proven to be popular among the control engineering community.

When the inverted pendulum is in upright position and the two wheeled mobile inverted pendulum doesn't move, the reference angle is set to zero ($\theta_{pref} = 0$). If the two wheeled mobile inverted pendulum moves forward, the reference angle is positive ($\theta_{pref} > 0$). If the two wheeled mobile inverted pendulum moves backward, the reference angle is negative ($\theta_{pref} < 0$).

A PD controller is designed to control the position of the two wheeled mobile inverted pendulum. Control law for PD controller can be as follows:

$$\begin{cases} e_x = x_{ref} - x_r \\ \theta_{pref} = K_{px} e_x + K_{dx} \dot{e}_x \end{cases} \quad (3.24)$$

where e_x is the displacement error of two wheeled mobile inverted pendulum, x_{ref} is the reference value for x_r , and K_{px} and K_{dx} are the proportional and derivative gains, respectively.

Chapter 4: Kalman Filter

4.1 Introduction

R.E Kalman published a paper in the early 1960s titled, “A New Approach to Linear Filtering and Prediction Problems.” R.E Kalman published his famous paper describing a solution to the discrete data linear filtering problem. Since the paper was published in the early 1960’s, the Kalman filter has become widely used in areas of embedded control systems and assisted navigation systems. As stated by both Greg Welch and Gary Bishop, “The Kalman filter is a set of mathematical equations that provides recursive solution to estimate the state of a process in a way that minimizes the mean of the squared error. The filter is very powerful in several aspects: it supports estimations of past, present, and even future states, and it can do so even when the precise nature of the modeled system is unknown.”

The Kalman filter has also gained popularity in others areas of engineering. The Kalman filter is often used in digital control engineering. The filter is used in control engineering to remove measurement noise that can affect the performance of system under control. It also provides an estimate of the current state of the process or system. As stated in the article, “Kalman Filtering” was written by Dan Simon, “The Kalman filter is a tool that can estimate the variables of a wide range of processes. In mathematical terms, we would say that a Kalman filter estimates the states of a linear system. Kalman filters are often implemented in embedded control systems because an accurate estimate of the process variables is needed in order to control a process.

After reviewing the articles on the Kalman filter, one can point out a major advantage of applying the filter to the two wheeled mobile inverted pendulum. The Kalman filter can be used to provide a good estimate of vertical angle to control and maintain the robot balance. It can also be used to remove any measurement noise from the inclinometer sensor. A disadvantage of the Kalman filter is that there is not a standard methodology or notation for the equations used for the filter and it makes the use of the filter more complex.

4.2 Kalman Filter Design

Most systems are described with continuous-time dynamics. However, state estimation and control algorithms are implemented in digital electronics field [27]. So, to design Kalman filter, firstly, the discrete stochastic system must be considered.

Eq. (2.34) and Eq. (2.35) must transform into linear dynamical discrete-time system as follows:

$$x(k+1) = Fx(k) + Gu(k) \quad (4.1)$$

$$y(k) = Hx(k) \quad (4.2)$$

$$F = e^{AT} \approx I + AT = \begin{bmatrix} 1 & T & 0 & 0 & 0 & 0 \\ 0 & 1 & \left(g + \left(\frac{\phi_1 \phi_2 g T}{M_p RL - \phi_1 \phi_2} \right) \right) & 0 & 0 & 0 \\ 0 & 0 & 1 & T & 0 & 0 \\ 0 & 0 & \left(\frac{-\phi_1 g T}{M_p RL - \phi_1 \phi_2} \right) & 1 & 0 & 0 \\ 0 & 0 & 0 & 0 & 1 & T \\ 0 & 0 & 0 & 0 & 0 & 1 \end{bmatrix} \quad (4.3)$$

$$G = e^{AT} \int_0^T e^{-At} dt B = A^{-1} (e^{AT} - I) B \approx BT$$

$$= \begin{bmatrix} 0 & 0 \\ \left(\frac{-\phi_2 T}{M_p RL - \phi_1 \phi_2} \right) & 0 \\ 0 & 0 \\ \left(\frac{T}{M_p RL - \phi_1 \phi_2} \right) & 0 \\ 0 & 0 \\ 0 & \left(\frac{T}{\phi_3} \right) \end{bmatrix} \quad (4.4)$$

$$H = C = \begin{bmatrix} 1 & 0 & 0 & 0 & 0 & 0 \\ 0 & 0 & 1 & 0 & 0 & 0 \\ 0 & 0 & 0 & 0 & 1 & 0 \end{bmatrix} \quad (4.5)$$

where T is sampling time

Proof of Eqs. (4.3) ~ (4.5) refers to Appendix A.

From Eqs. (4.1) and (4.2), the linear dynamical discrete-time system with the process noise and measurement noise becomes:

$$x(k+1) = Fx(k) + Gu(k) + v(k) \quad (4.6)$$

$$y(k) = Hx(k) + w(k) \quad (4.7)$$

The system state variable vector $x(k) \in \mathbb{R}^n$ denotes the full system state. The input variable vector $u(k) \in \mathbb{R}^m$ represents the two wheeled mobile inverted pendulum system input such as torque. The output variable vector $y(k) \in \mathbb{R}^p$ represents the system output measured by sensors such as pitch angle, rotation angle and moving displacement of system. The system matrix $F(k) \in \mathbb{R}^{n \times n}$ is a system matrix of the two wheeled mobile inverted pendulum system. $G(k) \in \mathbb{R}^{n \times m}$ is input matrix. The $v(k) \in \mathbb{R}^n$ is called the process noise vector and is assumed to be white Gaussian noise with zero mean and covariance matrix $V(k)$. The matrix $H(k) \in \mathbb{R}^{p \times m}$ is output matrix. The measurement noise vector, $w(k) \in \mathbb{R}^p$ is assumed to be white Gaussian noise with zero mean and covariance matrix, $W(k)$. It is assumed that $H(k)$ is full rank for all k although it may not be square.

The equations of Kalman filter can be decomposed into two groups: Time update and measurement update equations.

The time update equations use the current state and error covariance estimates to obtain estimates for the next time step.

Time Update (prediction)

$$\hat{x}_k^- = F\hat{x}_{k-1} + Gu_k \quad (4.8)$$

$$P_k^- = FP_{k-1}F^T + Q \quad (4.9)$$

where \hat{x}_k^- is predicted state and P_k^- is predicted covariance matrix.

Measurement Update

The measurement update equations use the current measurement to improve the estimates which are obtained from time update equations.

$$\begin{aligned}\hat{x}_k &= \hat{x}_k^- + K_k (z_k - H\hat{x}_k^-) \\ P_k &= (I - K_k H) P_k^- \\ K_k &= P_k^- H^T (H P_k^- H^T + R)^{-1}\end{aligned}\tag{4.10}$$

where \hat{x}_k is estimated state, K_k is Kalman gain, $(z_k - H\hat{x}_k^-)$ is error between prediction and measurement and P_k is update equation for covariance matrix.

In Kalman filter, the process noises are assumed to be white Gaussian noise with zero mean. The process noise vector is denoted as:

$$v(k) = \begin{bmatrix} \psi_1 \\ \psi_2 \\ \psi_3 \\ \psi_4 \\ \psi_5 \\ \psi_6 \end{bmatrix}\tag{4.11}$$

The covariance matrix of the process noise vector from Eq. (4.11) is

$$\begin{aligned}
V(k) &= \text{cov}(v(k)) = v(k)v(k)^T \\
&= \begin{bmatrix} \psi_1 \\ \psi_2 \\ \psi_3 \\ \psi_4 \\ \psi_5 \\ \psi_6 \end{bmatrix} \begin{bmatrix} \psi_1 & \psi_2 & \psi_3 & \psi_4 & \psi_5 & \psi_6 \end{bmatrix} \quad (4.12)
\end{aligned}$$

where, $\psi_1, \psi_2, \psi_3, \psi_4, \psi_5, \psi_6$ are process noises related to $x_r, \dot{x}_r, \theta_p, \dot{\theta}_p, \delta, \dot{\delta}$, respectively.

The measurement noise vector, $w(k)$, represents the noise that disturb the measurement process. The measurement noise vector is denoted as:

$$w(k) = \begin{bmatrix} \psi_7 \\ \psi_8 \\ \psi_9 \end{bmatrix} \quad (4.13)$$

The covariance matrix of the measurement noise vector from Eq. (4.13) is:

$$\begin{aligned}
W(k) &= \text{cov}(w(k)) = w(k)w(k)^T \\
&= \begin{bmatrix} \psi_7 \\ \psi_8 \\ \psi_9 \end{bmatrix} \begin{bmatrix} \psi_7 & \psi_8 & \psi_9 \end{bmatrix} \quad (4.14)
\end{aligned}$$

where, ψ_7, ψ_8, ψ_9 are measurement noises related to x_r, θ_p, δ , respectively.

4.3 Simulation Results

The purpose of this simulation is to verify the effectiveness of the Kalman filter reducing the effect of noise.

All parameters values and initial conditions for simulation are shown in Table 4.1.

Table 4.1 Parameter values and initial conditions

Parameters	Values	Units
M_p	26	[kg]
M_r	10.7	[kg]
D	0.566	[m]
L	0.14	[m]
g	9.81	[m/s ²]
J_r	0.8	[kgm ²]
J_δ	3.2	[kgm ²]
J_p	2.4	[kgm ²]
θ_{p0}	11.46	[degree]
x_{r0}	0	[m]
δ_0	0	[degree]
θ_{pref}	0	[degree]
x_{ref}	2	[m]
δ_{ref}	57	[degree]
R	0.22	[m]
T	0.01	[s]

The Kalman filter algorithm can be applied in the discrete time process of two wheeled mobile inverted pendulum system. For this simulation, process noise is omitted $v(k)=0$ and measurement noise vector is considered as:

$$w(k) = \begin{bmatrix} 0.09 \\ 0.22 \\ 0.06 \end{bmatrix} \quad (4.15)$$

Therefore, the covariance matrix of the measurement noise vector is:

$$W(k) = \begin{bmatrix} 0.0081 & 0.0198 & 0.0054 \\ 0.0198 & 0.0484 & 0.0132 \\ 0.0054 & 0.0132 & 0.0036 \end{bmatrix} \quad (4.16)$$



Fig. 4.1 shows the moving displacement of two wheeled mobile inverted pendulum in simulation with/without applying Kalman filter. There is noise in the moving displacement of system without applying Kalman filter. The noise is reduced significantly by using Kalman filter. Fig. 4.1 shows that the moving displacement of the system goes to reference displacement (2m) of the two wheeled mobile inverted pendulum after 7 seconds.

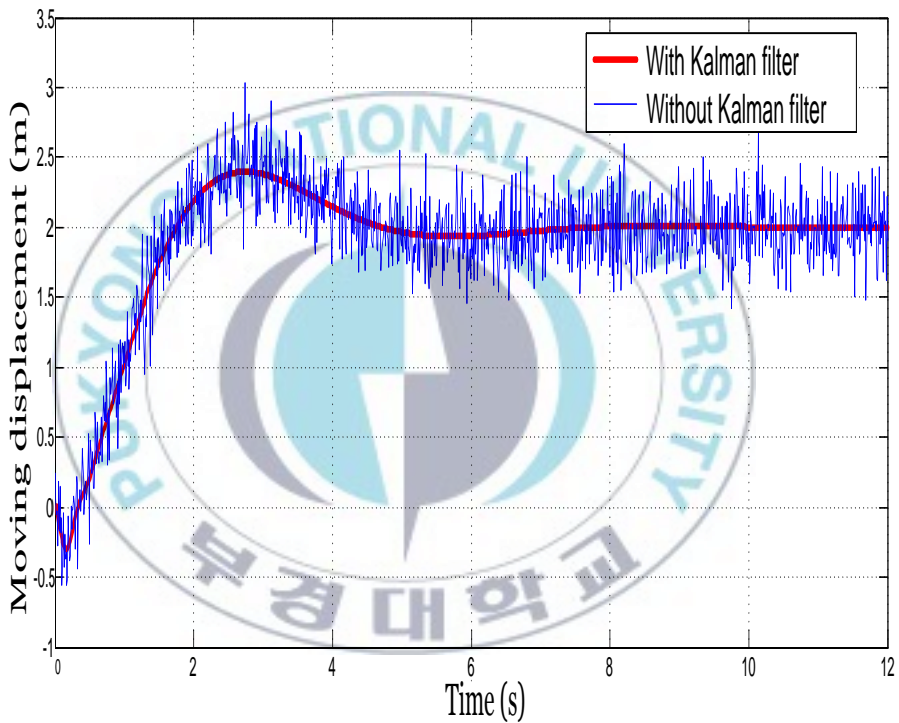


Fig. 4.1 Moving displacement x_r of system in simulation
with/without applying Kalman filter

Fig. 4.2 shows the pitch angle of the two wheeled mobile inverted pendulum system in simulation with/without applying Kalman filter. There is measurement noise in the pitch angle of system without applying Kalman filter. The noise is reduced significantly by using Kalman filter. The pitch angle goes to zero after 6 seconds.

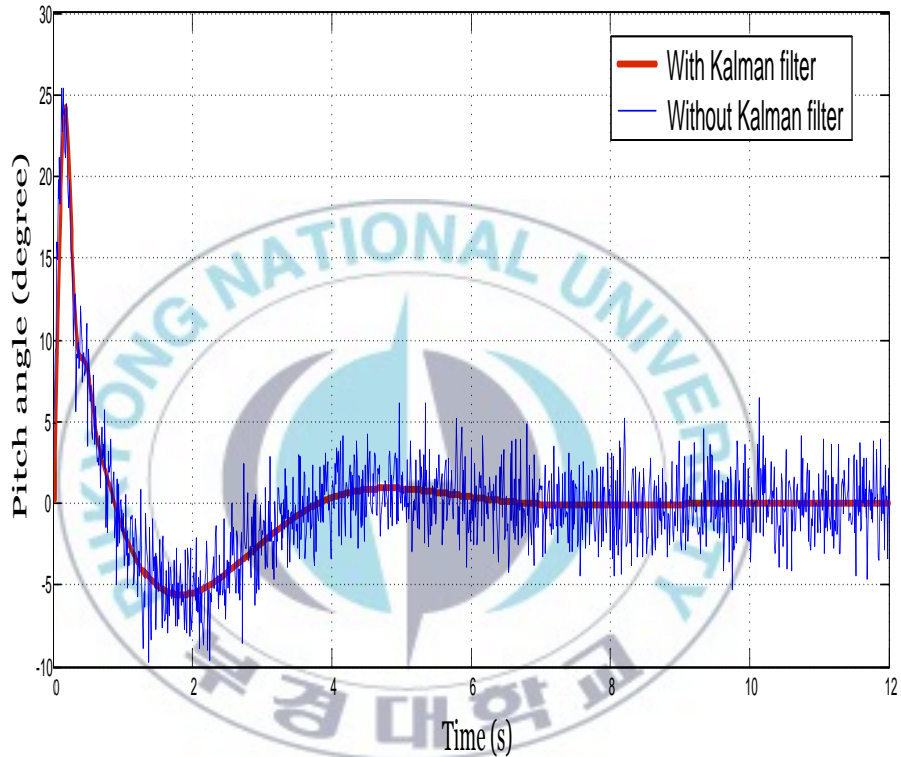


Fig. 4.2 Pitch angle θ_p in simulation with/without applying Kalman filter

Fig 4.3 shows the yaw angle of the two wheeled mobile inverted pendulum system in simulation with/without applying Kalman filter. There is measurement noise in the yaw angle of system without applying Kalman filter. The noise is reduced significantly by using Kalman filter. The yaw angle goes to reference yaw angle of two wheeled mobile inverted pendulum (57°) after 2 seconds.

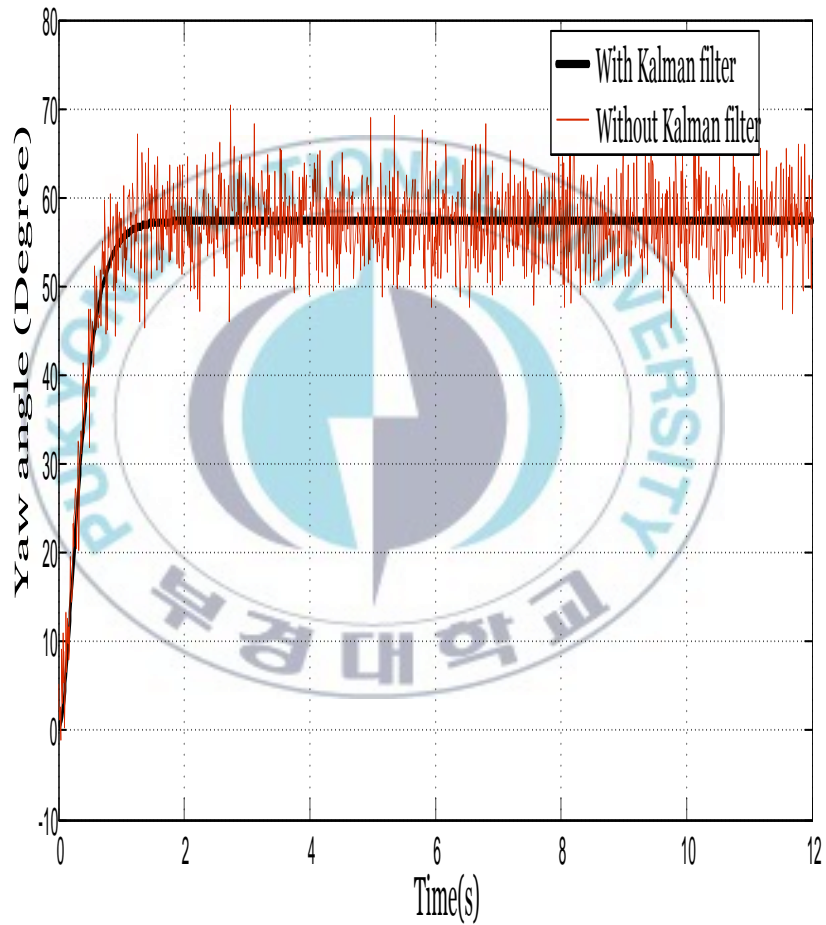


Fig. 4.3 Yaw angle δ in simulation with/without applying Kalman filter

To reduce the measurement noise of two wheeled mobile inverted pendulum system, Kalman filter is proposed. Based on the linear discrete-time system of two wheeled mobile inverted pendulum system, Kalman filter is designed. To verify the effectiveness of Kalman filter, the simulation is done. The simulation results show that the Kalman filter reduced the noise effectively.



Chapter 5: Simulations and Experimental results

5.1 Simulation Results

To verify the effectiveness of the proposed control system, simulations and experiments have been done for the two wheeled mobile inverted pendulum. The parameters and initial values of the two wheeled mobile inverted pendulum for the simulation and experimental are given in Table 5.1

Table 5.1 Numerical parameters and initial values for simulation

Parameters	Values	Units
M_p	26	[kg]
M_r	10.7	[kg]
D	0.566	[m]
L	0.14	[m]
g	9.81	[m/s ²]
J_r	0.8	[kgm ²]
J_δ	3.2	[kgm ²]
J_p	2.4	[kgm ²]
θ_{p0}	11.46	[degree]
x_{r0}	0	[m]
δ_0	0	[degree]
θ_{pref}	0	[degree]
x_{ref}	2	[m]
δ_{ref}	57	[degree]
R	0.22	[m]
T	0.01	[s]

The gains of backstepping controllers are determined with $k_1 = k_2 = 5$; $k_3 = k_4 = 5$ and the gains of PID controller is determined with $k_{px} = 0.14$ and $k_{dx} = 0.1$.

Fig. 5.1 shows the pitch angle θ_p of the two wheeled mobile inverted pendulum system in simulation result. The pitch angle θ_p goes to zero after 6 seconds.

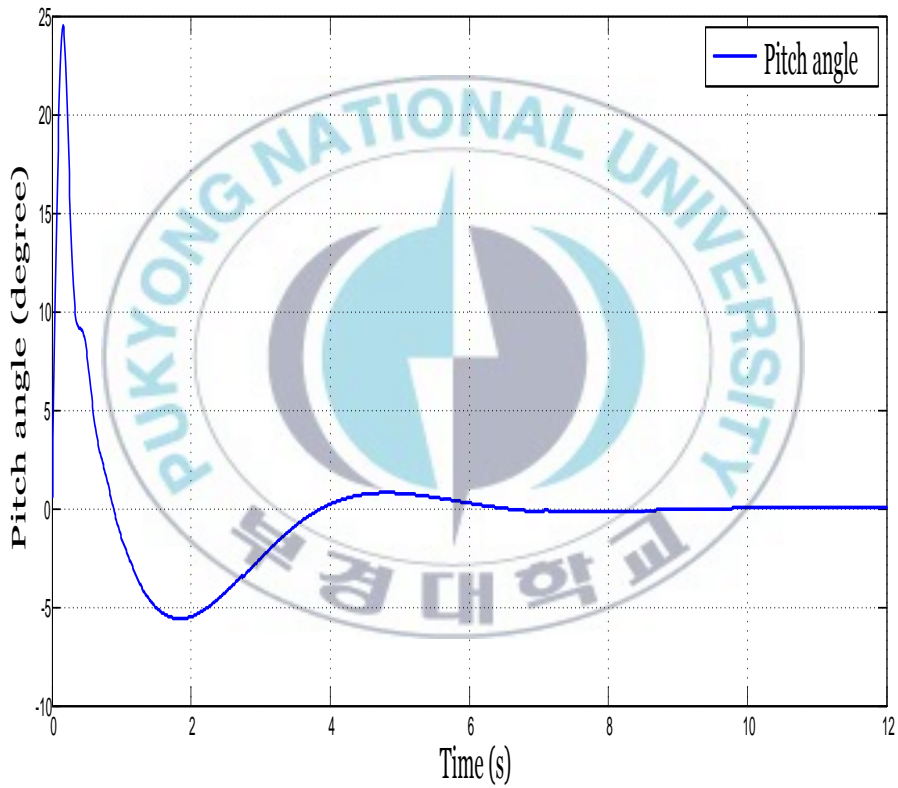


Fig. 5.1 Pitch angle θ_p in simulation result.

Fig. 5.2 shows the moving displacement x_r of the two wheeled mobile inverted pendulum at reference value assumed as zero. In simulation result, the moving displacement of the two wheeled mobile inverted pendulum reaches to reference moving displacement (2m) after 7 seconds.

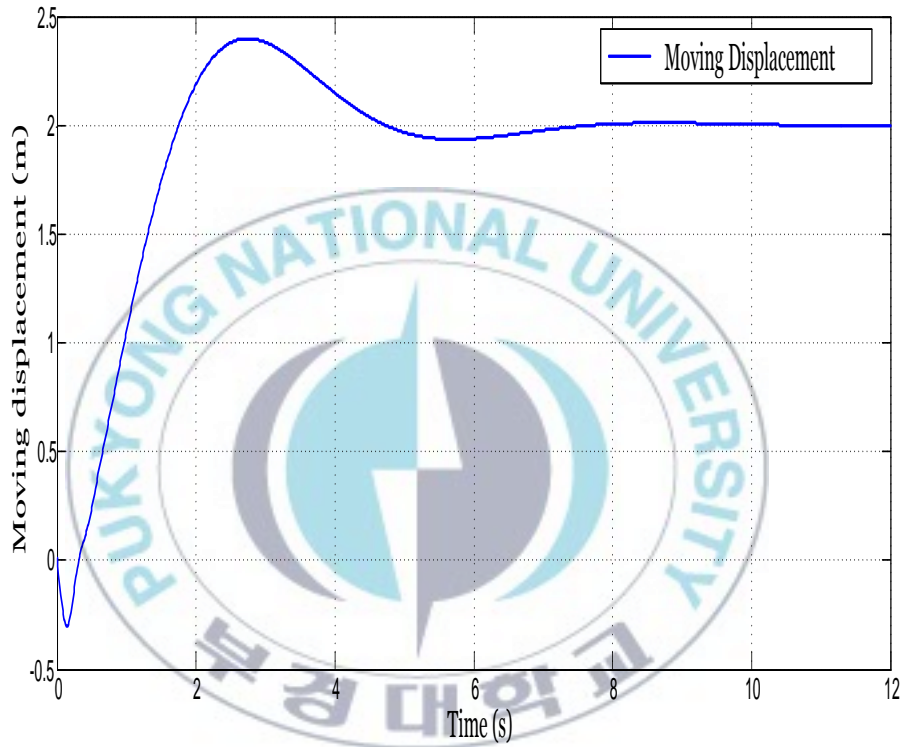


Fig. 5.2 Moving displacement x_r in simulation result

Fig. 5.3 shows the yaw angle δ of the two wheeled mobile inverted pendulum in simulation result. The yaw angle δ goes to the reference yaw angle (57°) after 2 seconds.

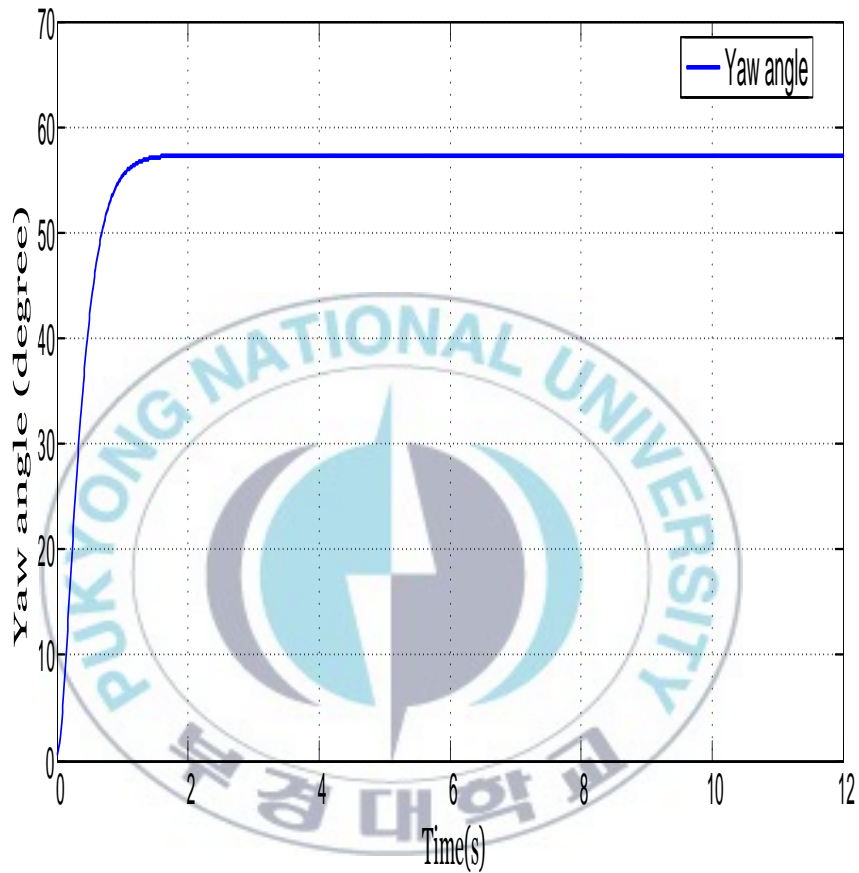


Fig. 5.3 Yaw angle δ in simulation result

5.2 Experimental Results

Fig. 5.4 shows the pitch angle θ_p of two wheeled inverted pendulum in experimental result with/without Kalman filter. Experimental result of the pitch angle with Kalman filter converges to 0.8° . Experimental result of the pitch angle without Kalman filter is bounded within $\pm 0.8^\circ$ around that with Kalman filter after 1.8 seconds.

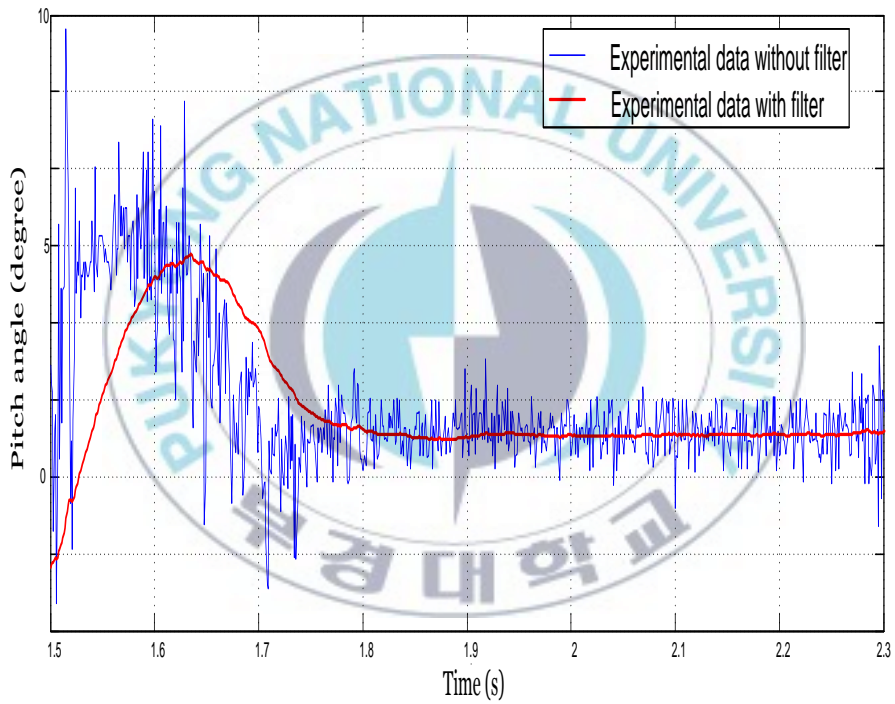


Fig. 5.4 Pitch angle θ_p with Kalman filter in experimental result

Fig. 5.5 shows the moving displacement of two wheeled mobile inverted pendulum in experiment. This shows that the two wheeled mobile inverted pendulum moves up to 2m and is then stabilized.



Fig. 5.5 Moving displacement of two wheel mobile inverted pendulum in experiment

Chapter 6: Conclusions and Future Works

6.1 Conclusions

This thesis presented controllers design method to stabilize and control the motion of the two wheeled mobile inverted pendulum. The two wheeled mobile inverted pendulum composed of chassis and base platform with two coaxial wheels. Conclusions of this thesis are given as follows:

- Linearized dynamic modeling of the two wheeled mobile inverted pendulum based on Newton's 2nd law is presented.
- Controller system via PD control and backstepping control is applied to stabilize and control the motion of two wheeled mobile inverted pendulum.
- To implement the proposed controller system for the two wheeled mobile inverted pendulum, the control system based on PIC18F452 microcontroller is developed. Encoders, inclinometer sensor and compass sensor are utilized to obtain the information of the system state.
- Kalman filter was proposed for estimating the moving displacement of two wheeled mobile inverted pendulum and pitch angle with sensor noise. The simulation results are shown to prove the effectiveness of proposed Kalman filter algorithm.

- The simulations and experimental results are shown to prove the effectiveness of the proposed model and controller system. In simulation results, the pitch angle of two wheeled mobile inverted pendulum is goes to stable after 6 seconds. Moving displacement in simulation goes to 2m after 7 seconds. Yaw angle of the two wheeled mobile inverted pendulum in simulation goes to reference yaw angle (57°) after 2 seconds. For the pitch angle θ_p to stabilize two wheeled inverted pendulum in experimental result with/without Kalman filter, experimental result of the pitch angle with Kalman filter converges to 0.8° . Experimental result of the pitch angle without Kalman filter is bounded within $\pm 0.8^\circ$ around that with Kalman filter after 1.8 seconds. Motion control for the moving displacement of two wheeled mobile inverted pendulum in experiment was shown. The two wheeled mobile inverted pendulum moves up to 2m and is then stabilized. So the proposed controller system can be applicable and implemented in practical to stabilize of the two wheeled mobile inverted pendulum.

6.2 Future Works

Some future works in the scope of this thesis are given as:

- The controller system developed in this thesis proved to be able to control the two wheeled mobile inverted pendulum. But the robustness of the system is not fully tested and is in question. More experiment needs to be performed to evaluate the robustness of the system and

fine tuning of the control algorithm is required for better performance. Future research on implementing non-linear controllers is strongly recommended to control the two wheeled mobile inverted pendulum system as it will improve the robustness of the system.

- Uneven field conditions can be considered for two wheeled mobile inverted pendulum.
- Experimental results of rotation control and position control will be shown.



References

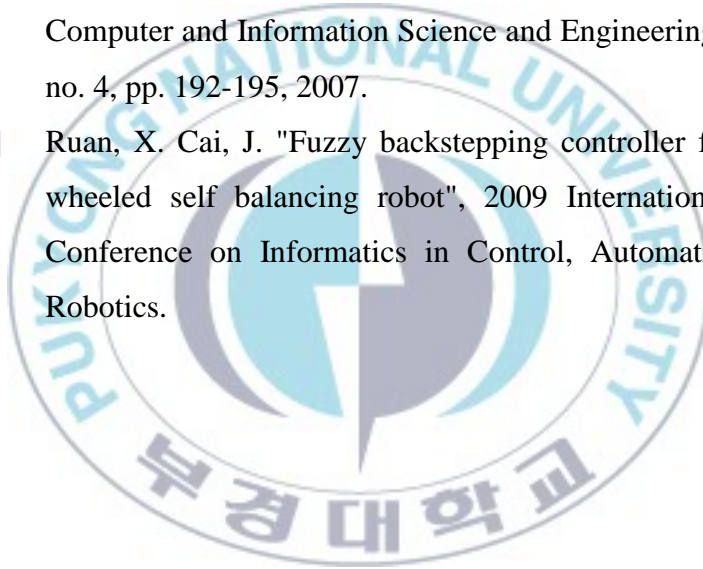
- [1] Li, J., Gao, X., Huang, Q., Du, Q., and Duan, X., “Mechanical design and dynamic modeling of a two-wheeled inverted pendulum mobile robot,” In Automation and Logistics, 2007 IEEE International Conference on, pp. 1614 - 1619, Aug. 2007.
- [2] Choi, D. and Oh, J. H., “Human friendly motion control of a wheeled inverted pendulum by reduced order disturbance observer,” in Robotics and Automation, 2008. ICRA 2008. IEEE International Conference on, pp. 2521 - 2526, May 2008.
- [3] Kim, Y., Kim, S. H., and Kwak, Y. K., “Dynamic analysis of a nonholonomic two-wheeled inverted pendulum robot,” Journal of Intelligent and Robotic Systems, vol. 44, pp. 25 - 46, 2005.
- [4] Katariya, A. S., “Optimal state-feedback and output-feedback controllers for the wheeled inverted pendulum system,” Master's thesis, Georgia Institute of Technology, 2010.
- [5] Ko, A., Lau, H., and Lau, T., “Soho security with mini self-balancing robots,” The Industrial Robot, vol. 32, no. 6, pp. 492 - 498, 2005.
- [6] Yamafuji, K. and Kawamura, T., “Study on the postural and driving control of a coaxial bicycle,” Transactions of the JSME, Series C, vol. 54, no. 501, pp. 1114 - 1121, 1988

- [7] Ha, Y.S. and Yuta, S., "Trajectory tracking control for navigation of the inverse pendulum type self-contained mobile robot," *Robotics and Autonomous Systems*, 1996.
- [8] Huang, J., Wang, H., Matsuno, T., Fukuda, T. and Sekiyama, K. "Robust velocity sliding mode control of mobile wheeled inverted pendulum systems," *IEEE International Conference on Robotics and Automation*, Japan, 2009.
- [9] Ding, F., Huang, J., Wang, Y., Matsuno, T., Fukuda, T., and Sekiyama, K., "Modeling and control of a novel narrow vehicle," In *Robotics and Biomimetics (ROBIO)*, 2010 *IEEE International Conference on*, pp. 1130 - 1135, Dec.2010.
- [10] Grasser, F., D'Arrigo, A., Colombi, S., and Rufer, A. C., "Joe: A mobile, inverted pendulum," *IEEE Transactions on Industrial Electronics*, vol. 49, pp. 107 - 114, Feb. 2002.
- [11] Sasaki, M., Yanagihara, N., Matsumoto, O., and Komoriya, K., "Forward and backward motion control of personal riding type wheeled mobile platform," in *Robotics and Automation*, 2004. *Proceedings. ICRA '04. 2004 IEEE International Conference on*, vol. 4, pp. 3331 – 3336, May 2004.
- [12] Salerno, A. and Angeles, J. "The control of semi-autonomous two wheeled robots is undergoing large payload variations," in *Proc. IEEE Int. Conf. Robot. Autom.*, pp. 1740–1745, Apr. 2004,
- [13] Segway Robotics, "Segway RMP," Accessed on Nov. 6, 2012. Available: <http://rmp.segway.com/>.

- [14] Baloh, M. and Parent, M. "Modeling and model verification of an intelligent self balancing two wheeled vehicle for an autonomous urban transportation system," in Proc. Conf. Comput. Intell. Robot. Auton. Syst., Singapore, Dec. 2003.
- [15] Benaskeur, A. and Desbiens, A. "Application of adaptive backstepping to the stabilization of the inverted pendulum," Electrical and Computer Engineering, 1998. IEEE Canadian Conference, vol. 1, pp. 113 - 116, May 1998,
- [16] Ming, T. K., Nguyen, T. P., Kim, H. K. and Kim, S. B. "Stabilizing control for nonlinear mobile inverted pendulum via sliding mode technique", Mechatronics, July 2007.
- [17] Pathak, K., Franch, J., and Agrawal, S. K., "Velocity and position control of a wheeled inverted pendulum by partial feedback linearization," IEEE Transactions on Robotics, vol. 21, no. 3, pp. 505 - 513, 2005.
- [18] Nawawi, S., Ahmad, M., and Osman, J., "Development of a two wheeled inverted pendulum mobile robot," In Research and Development, 2007. SCORED 2007. 5th Student Conference on, pp. 1 - 5, Dec. 2007.
- [19] Jeong, S. H. and Takahashi, T., "Wheeled inverted pendulum type assistant robot: inverted mobile, standing, and sitting motions," in Intelligent Robots and Systems, 2007. IROS 2007. IEEE/RSJ International Conference on, pp. 1932 - 1937, Nov. 2007.

- [20] Jung, S. and Kim, S. S., "Control experiment of a wheel-driven mobile inverted pendulum using neural network," *Control Systems Technology, IEEE Transactions on*, vol. 16, pp. 297 - 303, March 2008.
- [21] Li, Z. and Xu, C., "Adaptive fuzzy logic control of dynamic balance and motion for wheeled inverted pendulums," *Fuzzy Sets and Systems*, vol. 160, no. 12, pp. 1787 - 1803, 2009.
- [22] Vlassis, N., Toussaint, M., Kontes, G., and Piperidis, S., "Learning model free robot control by a Monte Carlo em algorithm," *Autonomous Robots*, vol. 27, pp. 123 - 130, 2009.
- [23] Huang, C., Wang, W.-J., and Chiu, C.-H., "Velocity control realization for a self-balancing transporter," *Control Theory Applications, IET*, vol. 5, pp. 1551 - 1560, Aug. 2011.
- [24] Bui, T. H., Nguyen, T. T., Chung, T. L., and Kim, S. B., "A simple nonlinear control of a two wheeled welding mobile robot," *International Journal of Control, Automation, and Systems*, vol. 1, no. 1, pp. 35 - 42, 2003.
- [25] Li, Z. and Zhang, Y., "Robust adaptive motion force control for wheeled inverted pendulums," *Automatica*, vol. 46, no. 8, pp. 1346 - 1353, 2010.
- [26] Thao, N. G. M., Nghia, D. H., Phuc, N. H., "A PID backstepping controller for two wheeled self-balancing robot," *International Forum on Strategic Technology (IFOST)*, pp. 76 – 81, South Korea, 2010

- [27] Ogata, K. "Discrete-time control systems", Prentice-Hall Inc., New Jersey, 1995.
- [28] Choi, N. S., Kim, S. K., Lee, G. Y., Kim, H. K. and Kim, S. B., "Sliding mode controller design for rejecting disturbance of mobile inverted pendulum", Proceedings of the 11th Conference on Science and Technology, pp 169 – 174, 2009
- [29] Altinöz, Ö. T. , "Adaptive integral backstepping motion control for inverted pendulum," International Journal of Computer and Information Science and Engineering, vol. 1, no. 4, pp. 192-195, 2007.
- [30] Ruan, X. Cai, J. "Fuzzy backstepping controller for two-wheeled self balancing robot", 2009 International Asia Conference on Informatics in Control, Automation and Robotics.



Publications and Conferences

A. Conferences

- [1] Phuc Thinh Doan, **Chetanraj Patil**, Hak Kyeong Kim, Sang Bong Kim, “Motion control of Segway vehicle using PID backstepping control method”, *International Symposium On Mechatronics And Robotics*, Hochiminh City University Of Technology, Ho Chi Minh City, Vietnam, **Oct 2011**.
- [2] Phuc Thinh Doan, **Chetanraj Patil**, Hak Kyeong Kim, Sang Bong Kim. “PID Backstepping controller design for motion control of Segway vehicle”, *ISAMPE 2011 International Symposium On Advanced Mechanical And Power Engineering(10-13 Nov. 2011)*, Pukyong National University, Busan, Republic of Korea, **Nov 2011**.
- [3] **Chetanraj Patil**, Pandu Sandi Pratama, Hak Kyeong Kim, Sang Bong Kim. “Control of two wheeled mobile inverted pendulum using Kalman filter and backstepping controller”, *ISAMPE 2012 International Symposium On Advanced Mechanical And Power Engineering (8-10 Nov. 2012)*, University of Shanghai for Science and Technology, Shanghai, China, **Nov 2012**.

APPENDIX A

Discretization

Exponential function has the following relationship:

$$e^{At} = I + At + \frac{1}{2!} A^2 t^2 + \dots + \frac{1}{n!} A^n t^n + \dots = \sum_{n=0}^{\infty} \frac{A^n t^n}{n!} \quad (\text{A.1})$$

$$\begin{aligned} \frac{d}{dt} e^{At} &= A + A^2 t + \frac{A^3 t^2}{2!} + \dots + \frac{A^n t^{n-1}}{(n-1)!} + \dots \\ &= A \left[I + At + \frac{A^2 t^2}{2!} + \dots + \frac{A^{n-1} t^{n-1}}{(n-1)!} + \dots \right] = A e^{At} \end{aligned} \quad (\text{A.2})$$

A continuous time state equation and output equation are:

$$\dot{x}(t) = Ax(t) + Bu(t) \quad (\text{A.3})$$

$$y(t) = Cx(t) \quad (\text{A.4})$$

From Eq. (A.3), the following is obtained:

$$\dot{x}(t) - Ax(t) = Bu(t) \quad (\text{A.5})$$

Multiplying e^{-At} both sides of Eq. (A.5) yields:

$$e^{-At} [\dot{x}(t) - Ax(t)] = \frac{d}{dt} [e^{-At} x(t)] = e^{-At} Bu(t) \quad (\text{A.6})$$

Integrating Eq. (A.5) between 0 and t gives:

$$e^{-At} x(t) = x(0) + \int_0^t e^{-A\tau} Bu(\tau) d\tau \quad (\text{A.7})$$

Therefore, solution of continuous time state equation of Eq. (A.3) is:

$$\begin{aligned}
x(t) &= e^{At} x(0) + \int_0^t e^{A(t-\tau)} Bu(\tau) d\tau \\
&= e^{At} x(0) + e^{At} \int_0^t e^{-A\tau} Bu(\tau) d\tau
\end{aligned} \tag{A.8}$$

Discrete time state equation of Eq. (A.8) putting $t = kT$, $u(t) = u(kT)$ for $kT \leq t \leq kT + T$ is obtained as,

$$x(kT) = e^{AkT} x(0) + e^{AkT} \int_0^{kT} e^{-A\tau} Bu(\tau) d\tau \tag{A.9}$$

For $t = (k+1)T$, the following is obtained from Eq. (A.8).

$$x((k+1)T) = e^{A(k+1)T} x(0) + e^{A(k+1)T} \int_0^{(k+1)T} e^{-A\tau} Bu(\tau) d\tau \tag{A.10}$$

Multiplying e^{AT} in the both side of Eq. (A.9) and subtracting it from Eq. (A.10) gives:

$$x((k+1)T) = e^{AT} x(kT) + e^{A(k+1)T} \int_{kT}^{(k+1)T} e^{-A\tau} Bu(\tau) d\tau \tag{A.11}$$

From discrete-time state equation of Eq. (A.11) that $u(\tau) = u(kT)$, $x(0)$ is the value of the state at time $t = t_0 = 0$, and $x(k)$ is the value of the state at time $t_0 + Tk$, and $t = \tau - kT$ and T is defined to be the sampling time, the following is obtained:

$$\begin{aligned}
x((k+1)T) &= e^{AT} x(kT) + e^{AT} \int_0^T e^{-At} Bu(kT) dt \\
&= e^{AT} x(kT) + \int_0^T e^{A(T-t)} B dt u(kT)
\end{aligned} \tag{A.12}$$

Eqs. (A.3) and (A.4) can be expressed ad a discrete time system as follows:

$$x(k+1) = Fx(k) + Gu(k) \tag{A.13}$$

$$y(k) = Hx(k) \tag{A.14}$$

If Eq. (A.13) and (A.14) compared to Eqs. (A.4) and (A.12), respectively, the following is obtained:

$$F = e^{AT} \quad (\text{A.15})$$

$$G = \left(\int_0^T e^{A(T-t)} \right) B dt = A^{-1} (e^{AT} - I) B \quad (\text{A.16})$$

$$H = C \quad (\text{A.17})$$

Using Taylor series, Eqs. (A.15) and (A.16) are reduced as:

$$F = e^{AT} = I + AT + \frac{A^2 T^2}{2!} + \frac{A^3 T^3}{3!} + \dots + \frac{A^n T^n}{n!} \dots \quad (\text{A.18})$$

$$G = \int_0^T e^{A(T-t)} dt B = - \int_T^0 e^{A\tau} d\tau B = \int_0^T e^{A\tau} d\tau B \quad (\text{A.19})$$

$$= \left[A\tau + \frac{A^2 \tau^2}{2!} + \frac{A^3 \tau^3}{3!} + \dots + \frac{A^n \tau^n}{n!} \dots \right]_0^T B$$

$$= A^{-1} \left[AT + \frac{A^2 T^2}{2!} + \frac{A^3 T^3}{3!} + \dots + \frac{A^n T^n}{n!} \dots \right] B \quad (\text{A.20})$$

$$= A^{-1} [e^{AT} - I] B \quad (\text{A.21})$$

where $\tau = T - t$ and $-dt = d\tau$

Eqs. (A.18) and (A.20) taking $n = 1$ becomes

$$F = e^{AT} = I + AT \quad (\text{A.22})$$

$$G = A^{-1} [AT] B = TB \quad (\text{A.23})$$

Using Eqs. (A.22) and (A.23), the discrete time equations of two wheeled mobile inverted pendulum are obtained as follows:

$$x(k+1) = (I + AT)x(k) + BTu(k) \quad (\text{A.24})$$

$$\begin{aligned}
& \left[\begin{array}{cccccc} 1 & 0 & 0 & 0 & 0 & 0 \\ 0 & 1 & 0 & 0 & 0 & 0 \\ 0 & 0 & 1 & 0 & 0 & 0 \\ 0 & 0 & 0 & 1 & 0 & 0 \\ 0 & 0 & 0 & 0 & 1 & 0 \\ 0 & 0 & 0 & 0 & 0 & 1 \end{array} \right] + \\
& = \left[\begin{array}{cccccc} 0 & 1 & & 0 & & 0 \\ 0 & 0 & \left(g + \left(\frac{\phi_1 \phi_2 g}{M_p RL - \phi_1 \phi_2} \right) \right) & & 0 & 0 \\ 0 & 0 & & 0 & 1 & 0 \\ 0 & 0 & \left(\frac{-\phi_1 g}{M_p RL - \phi_1 \phi_2} \right) & & 0 & 0 \\ 0 & 0 & & 0 & 0 & 1 \\ 0 & 0 & & 0 & 0 & 0 \end{array} \right] x(k) \\
& + \left[\begin{array}{c} 0 \\ \left(\frac{-\phi_2}{M_p RL - \phi_1 \phi_2} \right) \\ 0 \\ \left(\frac{1}{M_p RL - \phi_1 \phi_2} \right) \\ 0 \\ 0 \end{array} \right] Tu(k) \\
& \left[\begin{array}{c} 0 \\ 0 \\ 0 \\ 0 \\ 0 \\ \left(\frac{1}{\phi_3} \right) \end{array} \right]
\end{aligned} \tag{A.25}$$

$$= \begin{bmatrix} 1 & T & 0 & 0 & 0 & 0 \\ 0 & 1 & \left(g + \left(\frac{\phi_1 \phi_2 g T}{M_p R L - \phi_1 \phi_2} \right) \right) & 0 & 0 & 0 \\ 0 & 0 & 1 & T & 0 & 0 \\ 0 & 0 & \left(\frac{-\phi_1 g T}{M_p R L - \phi_1 \phi_2} \right) & 1 & 0 & 0 \\ 0 & 0 & 0 & 0 & 1 & T \\ 0 & 0 & 0 & 0 & 0 & 1 \end{bmatrix} x(k) \quad (A.26)$$

$$+ \begin{bmatrix} 0 & 0 \\ \left(-\phi_2 T / M_p R L - \phi_1 \phi_2 \right) & 0 \\ 0 & 0 \\ \left(T / M_p R L - \phi_1 \phi_2 \right) & 0 \\ 0 & 0 \\ 0 & \left(T / \phi_3 \right) \end{bmatrix} u(k)$$

$= Fx(k) + Gu(k)$

$$y(k) = Hx(k) = Cx(k) = \begin{bmatrix} 1 & 0 & 0 & 0 & 0 & 0 \\ 0 & 0 & 1 & 0 & 0 & 0 \\ 0 & 0 & 0 & 0 & 1 & 0 \end{bmatrix} x(k) \quad (A.27)$$

From Eqs. (A.26) ~ (A.28), the following are obtained.

$$\begin{aligned}
 F &= \begin{bmatrix} 1 & T & 0 & 0 & 0 & 0 \\ 0 & 1 & \left(g + \left(\frac{\phi_1 \phi_2 g T}{M_p R L - \phi_1 \phi_2} \right) \right) & 0 & 0 & 0 \\ 0 & 0 & 1 & T & 0 & 0 \\ 0 & 0 & \left(\frac{-\phi_1 g T}{M_p R L - \phi_1 \phi_2} \right) & 1 & 0 & 0 \\ 0 & 0 & 0 & 0 & 1 & T \\ 0 & 0 & 0 & 0 & 0 & 1 \end{bmatrix} \\
 G &= \begin{bmatrix} 0 & 0 \\ \left(-\phi_2 T / M_p R L - \phi_1 \phi_2 \right) & 0 \\ 0 & 0 \\ \left(T / M_p R L - \phi_1 \phi_2 \right) & 0 \\ 0 & 0 \\ 0 & \left(T / \phi_3 \right) \end{bmatrix} \\
 H &= \begin{bmatrix} 1 & 0 & 0 & 0 & 0 & 0 \\ 0 & 0 & 1 & 0 & 0 & 0 \\ 0 & 0 & 0 & 0 & 1 & 0 \end{bmatrix}
 \end{aligned} \tag{A.28}$$